Optimization of Large Setups

Using machine learning

Denis Derkach

LAMBDA, HSE University, Moscow, Russia

LAMBDA • HSE

02 November 2022

Why Optimization?

- Optimization is a question of survival.
- Industrial equipment can be optimized for:
  - Lower costs.
  - Less emission.
  - Faster production.
  - Etc.
- Need digital twin of the setup for better tuning.

Surrogate modeling in a wild

Surrogate Models

- Model
  - Computational (e.g. Computational Fluid Dynamics)
  - Data–driven
- Goals
  - Design optimization
  - Configuration space approximation
- Most critical task:
  - A strategy for using the surrogates is known as model management.

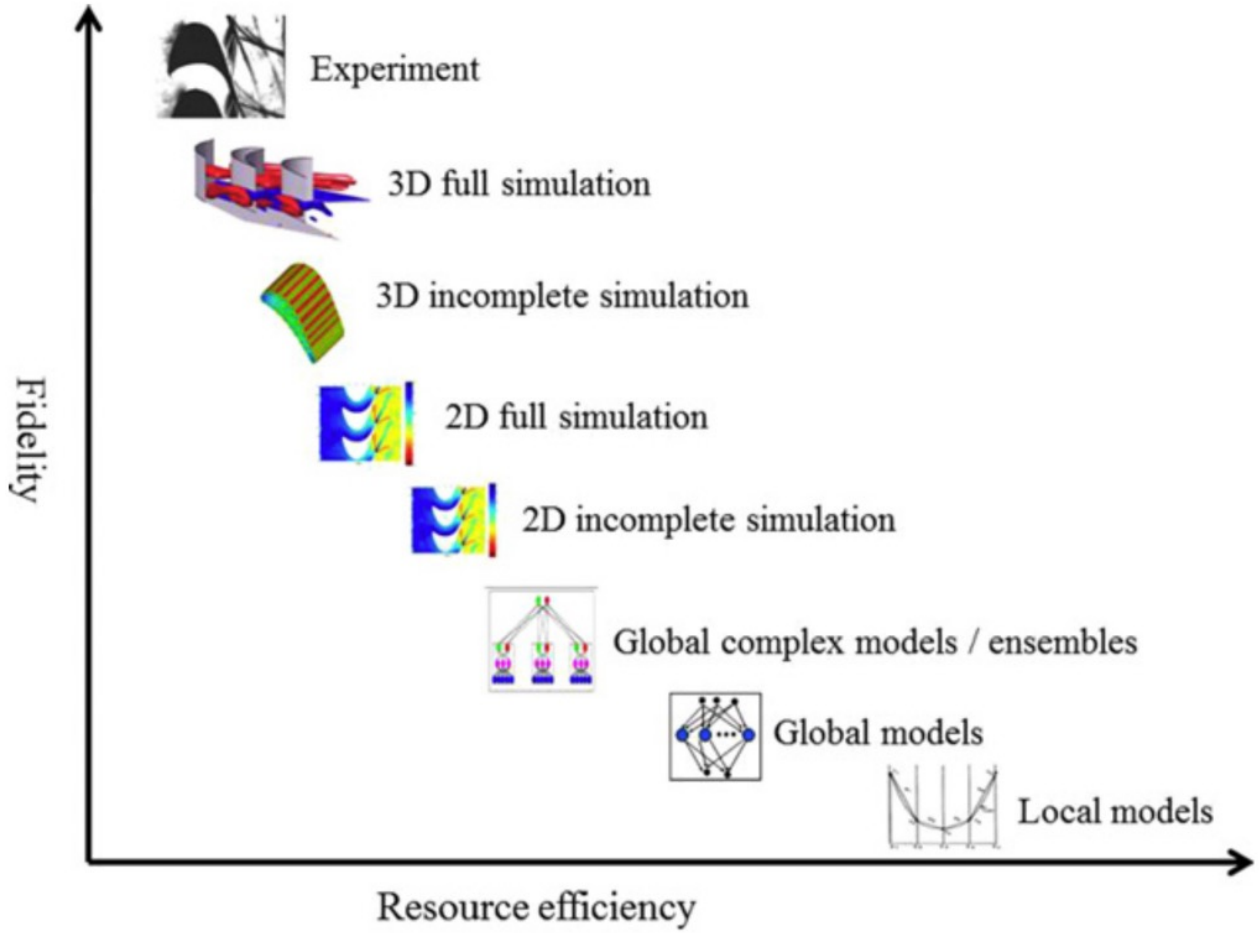

Why Bother

- Examples
  - Drug design
  - Aero engineering (aircraft wing profile, turbine)
  - Steel production quality control
  - Weather forecasting
- Regular physically-based computational models are fine but
  - Expensive computation
  - Large parameter space
  - Numerical noise / uncertainty

Surrogate Modelling. Generic Optimization

- How to construct surrogate?
- What if the surrogate needs CPU intensive resources?

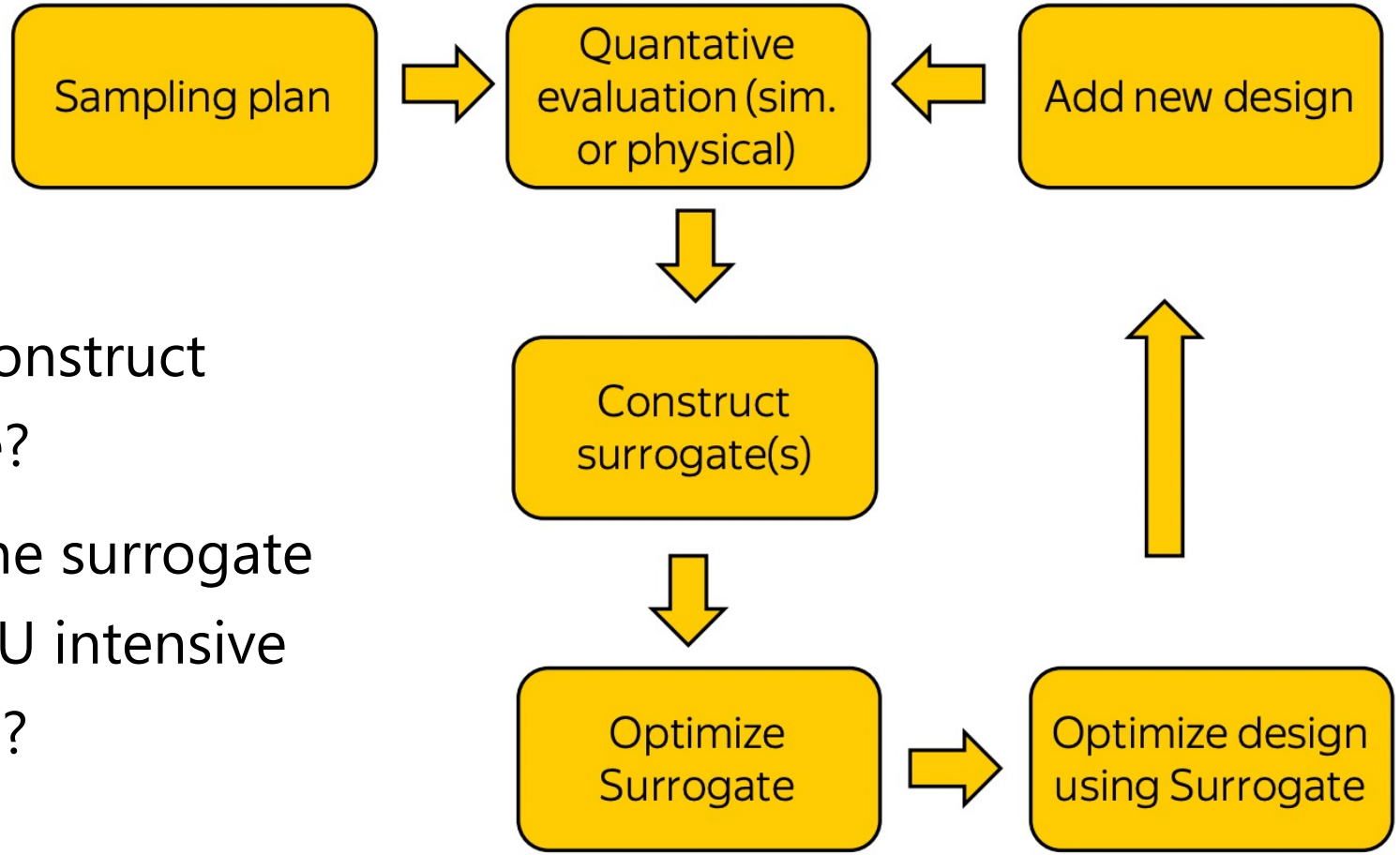

Surrogate Modelling. Generic Optimization

Polynomial

Radial Basis Functions (RBF)

$$\widehat{f}\left(\mathbf{x}^{(j)}\right) = \sum_{i=1}^{n_c} w_i \psi(\|\mathbf{x}^{(j)} - \mathbf{c}^{(i)}\|) = y^{(j)}, \quad j = 1, \ldots, n$$

- Gaussian $\psi(r) = \mathrm{e}^{-r^2/(2\sigma^2)}$
- multiquadric $\psi(r) = (r^2 + \sigma^2)^{1/2}$
- inverse multiquadric $\psi(r) = (r^2 + \sigma^2)^{-1/2}$

Neural Networks

Kriging / Gaussian Processes

$$\psi^{(i)} = \exp\left(-\sum_{j=1}^{k} \theta_j \mid x_j^{(i)} - x_j \mid^{p_j}\right)$$

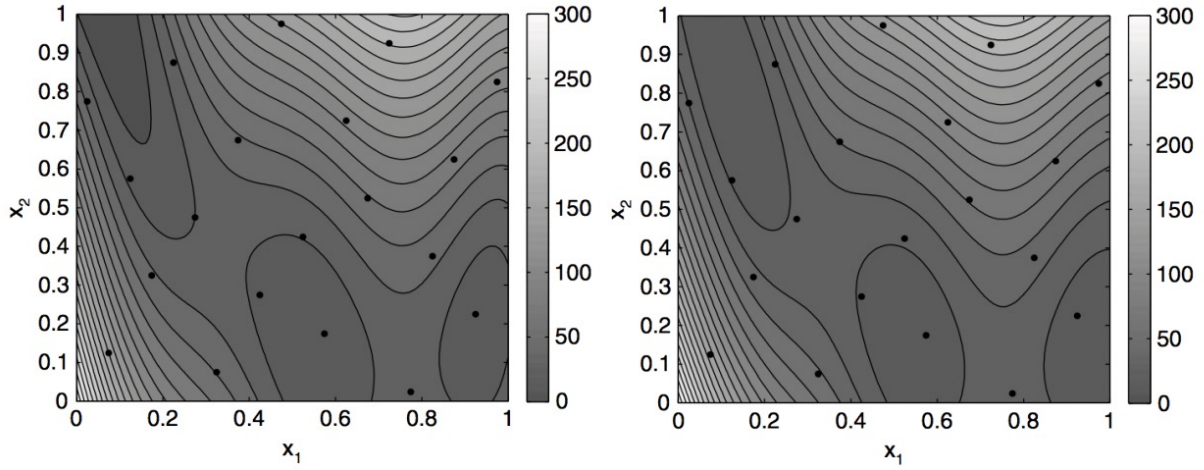

Kriging over Branin function after 20 iterations

The Collider

Collider

Large Hadron Collider

- Millions of events per second.
- Underlying models govern collision outcome.
- Hypotheses testing for theories that describe models.
- Higgs Boson.

Large Hadron Collider

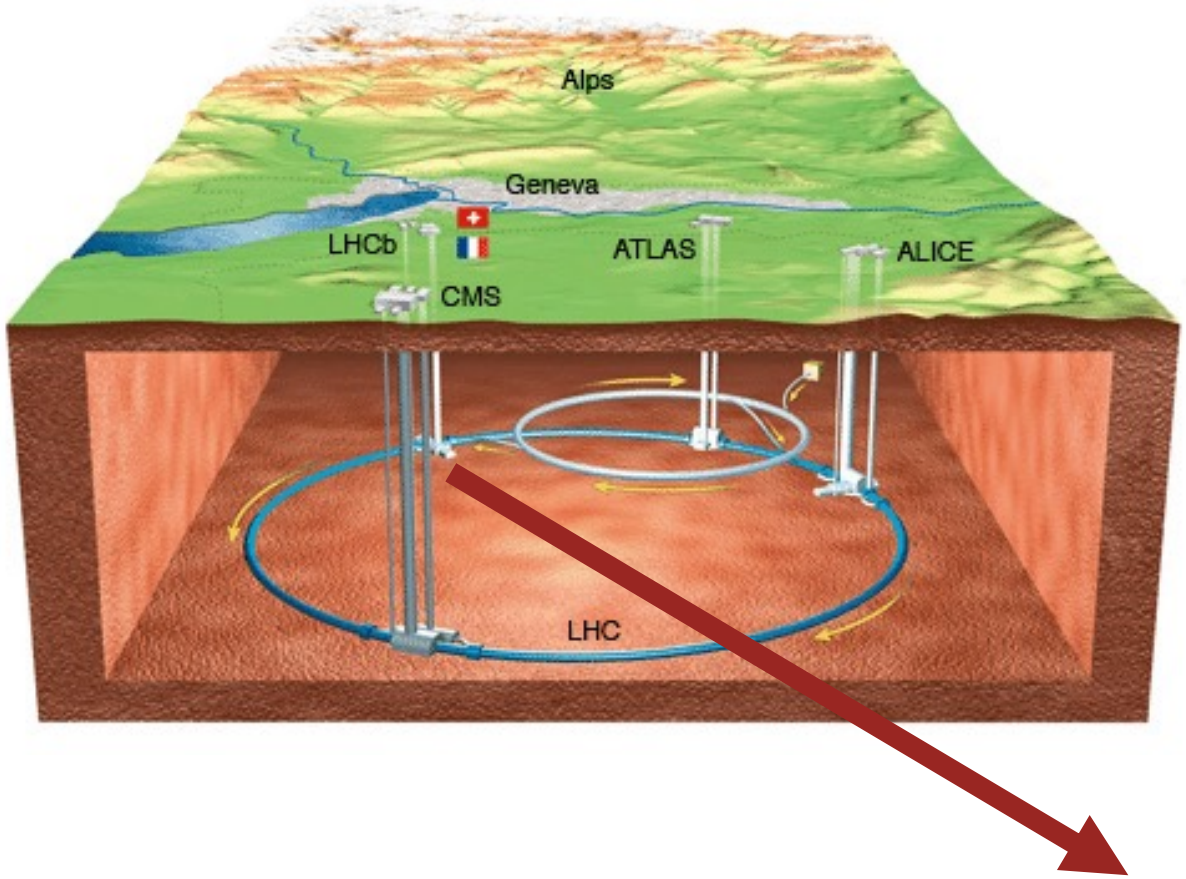

"Cameras" under the surface:

- many layers of sensors: ~200 sq.m. matrices
- resolution: ~100M pixels
- photo speed: 40 000 000 events per second
- record: 200-1000 photos per second
- work for many years

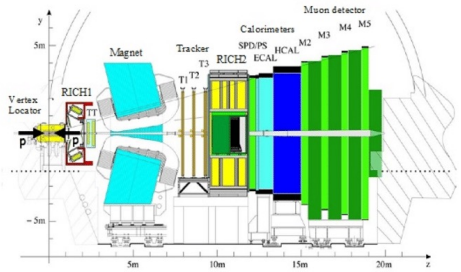

Detector Proper

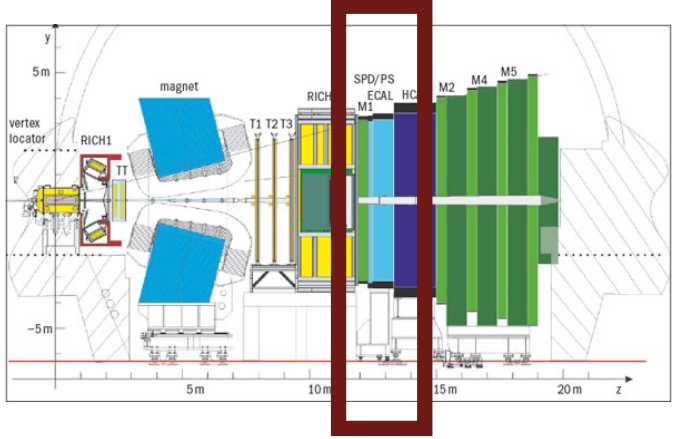

Size: 7.8x6.3x0.5 m

Module size 12x12 cm^2

176 inner modules: 9 cells with size 4x4 cm^2
448 middle modules: 4 cells with size 6x6 cm^2
2688 outer modules: 1 cell with size 12x12 cm^2

LHC: Machine Learning

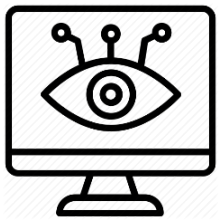

Monitoring

Simulation

Hardware trigger (L0)

- Real-time
- Selects events with hits in muon chamber
- Selects events with significant amount of transverse energy in hadronic calorimeter

Software trigger 1 (HLT1)

- Real-time
- Selects events with muons
- Selects event s with high $p\downarrow t$ tracks
- Selects events with high IP

Software trigger 2 (HLT2)

- Complete event reconstruction
- Decay-specific selection

Offline reconstruction

Analysis

- Decay-specific user-specific

https://pos.sissa.it/321/226/pdf

LHC: Machine Learning

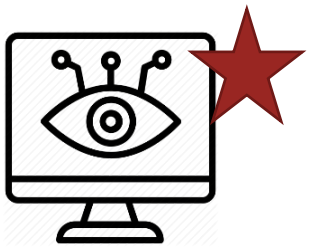

Monitoring

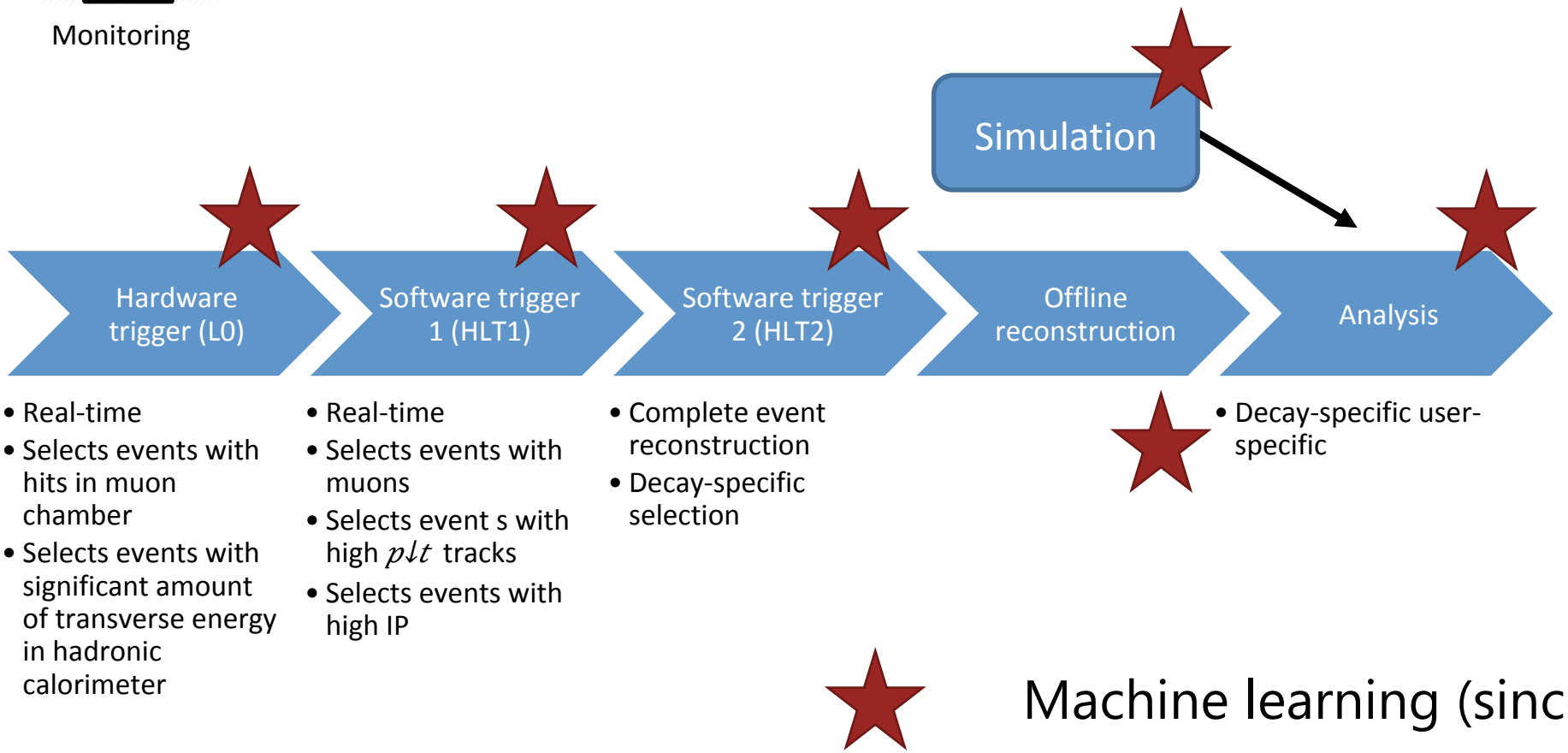

Machine learning (since 1993)

https://pos.sissa.it/321/226/pdf

Tuning

Theory Construction

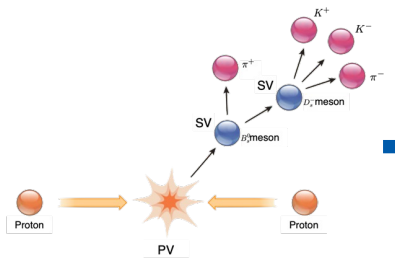

$$\mathcal{L}_{GWS} = \sum_f (\bar{\Psi}_f (i\gamma^\mu \partial\mu - m_f)\Psi_f - eQ_f \bar{\Psi}_f \gamma^\mu \Psi_f A_\mu) +$$

$$+\frac{g}{\sqrt{2}} \sum_i (\bar{a}_L^i \gamma^\mu b_L^i W_\mu^+ + \bar{b}_L^i \gamma^\mu a_L^i W_\mu^-) + \frac{g}{2c_w} \sum_f \bar{\Psi}_f \gamma^\mu (I_f^3 - 2s_w^2 Q_f - I_f^3 \gamma_5) \Psi_f Z_\mu +$$

$$-\frac{1}{4}|\partial_\mu A_\nu - \partial_\nu A_\mu - ie(W_\mu^- W_\nu^+ - W_\mu^+ W_\nu^-)|^2 - \frac{1}{2}|\partial_\mu W_\nu^+ - \partial_\nu W_\mu^+ +$$

$$-ie(W_\mu^+ A_\nu - W_\nu^+ A_\mu) + ig' c_w (W_\mu^+ Z_\nu - W_\nu^+ Z_\mu|^2 +$$

$$-\frac{1}{4}|\partial_\mu Z_\nu - \partial_\nu Z_\mu + ig' c_w (W_\mu^- W_\nu^+ - W_\mu^+ W_\nu^-)|^2 +$$

$$-\frac{1}{2} M_\eta^2 \eta^2 - \frac{g M_\eta^2}{8 M_W} \eta^3 - \frac{g'^2 M_\eta^2}{32 M_W} \eta^4 + |M_W W_\mu^+ + \frac{g}{2} \eta W_\mu^+|^2 +$$

$$+\frac{1}{2}|\partial_\mu \eta + i M_Z Z_\mu + \frac{ig}{2c_w} \eta Z_\mu|^2 - \sum_f \frac{g}{2} \frac{m_f}{M_W} \bar{\Psi}_f \Psi_f \eta$$

Data collection

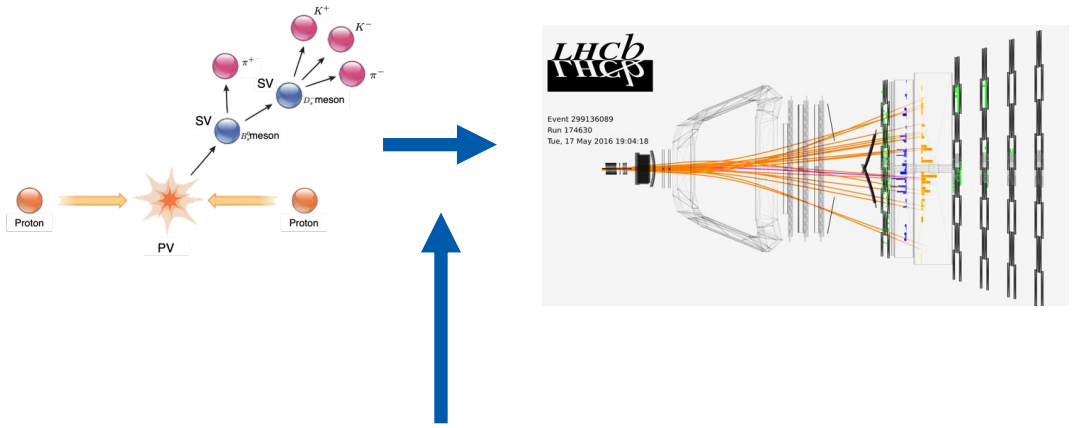

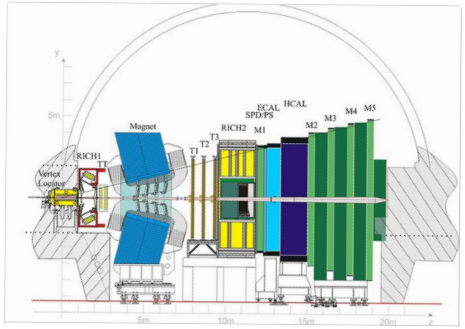

Data Collection

$$\mathcal{L}_{GWS} = \sum_f (\bar{\Psi}_f (i\gamma^\mu \partial\mu - m_f)\Psi_f - eQ_f \bar{\Psi}_f \gamma^\mu \Psi_f A_\mu) +$$
$$+ \frac{g}{\sqrt{2}} \sum_i (\bar{a}_L^i \gamma^\mu b_L^i W_\mu^+ + \bar{b}_L^i \gamma^\mu a_L^i W_\mu^-) + \frac{g}{2c_w} \sum_f \bar{\Psi}_f \gamma^\mu (I_f^3 - 2s_w^2 Q_f - I_f^3 \gamma_5) \Psi_f Z_\mu +$$
$$- \frac{1}{4} |\partial_\mu A_\nu - \partial_\nu A_\mu - ie(W_\mu^- W_\nu^+ - W_\mu^+ W_\nu^-)|^2 - \frac{1}{2} |\partial_\mu W_\nu^+ - \partial_\nu W_\mu^+ +$$
$$- ie(W_\mu^+ A_\nu - W_\nu^+ A_\mu) + ig' c_w (W_\mu^+ Z_\nu - W_\nu^+ Z_\mu|^2 +$$
$$- \frac{1}{4} |\partial_\mu Z_\nu - \partial_\nu Z_\mu + ig' c_w (W_\mu^- W_\nu^+ - W_\mu^+ W_\nu^-)|^2 +$$
$$- \frac{1}{2} M_\eta^2 \eta^2 - \frac{g M_\eta^2}{8 M_W} \eta^3 - \frac{g'^2 M_\eta^2}{32 M_W} \eta^4 + |M_W W_\mu^+ + \frac{g}{2} \eta W_\mu^+|^2 +$$
$$+ \frac{1}{2} |\partial_\mu \eta + i M_Z Z_\mu + \frac{ig}{2c_w} \eta Z_\mu|^2 - \sum_f \frac{g}{2} \frac{m_f}{M_W} \bar{\Psi}_f \Psi_f \eta$$

Data reconstruction

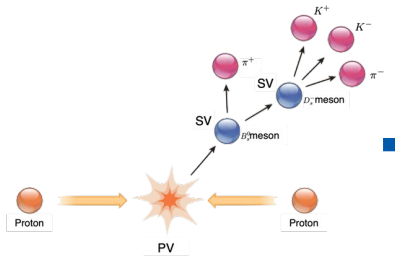

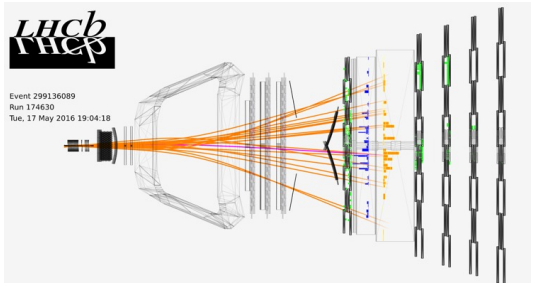

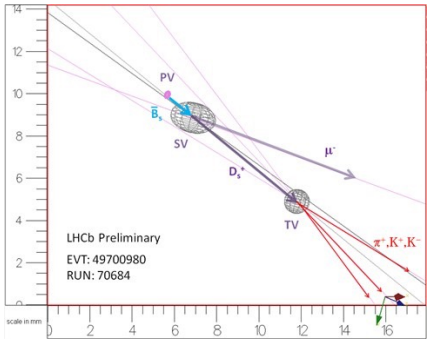

$$\mathcal{L}_{GWS} = \sum_f (\bar{\Psi}_f (i\gamma^\mu \partial\mu - m_f)\Psi_f - eQ_f \bar{\Psi}_f \gamma^\mu \Psi_f A_\mu) +$$
$$+\frac{g}{\sqrt{2}} \sum_i (\bar{a}^i_L \gamma^\mu b^i_L W^+_\mu + \bar{b}^i_L \gamma^\mu a^i_L W^-_\mu) + \frac{g}{2c_w} \sum_f \bar{\Psi}_f \gamma^\mu (I^3_f - 2s^2_w Q_f - I^3_f \gamma_5) \Psi_f Z_\mu +$$
$$-\frac{1}{4}|\partial_\mu A_\nu - \partial_\nu A_\mu - ie(W^-_\mu W^+_\nu - W^+_\mu W^-_\nu)|^2 - \frac{1}{2}|\partial_\mu W^+_\nu - \partial_\nu W^+_\mu +$$
$$-ie(W^+_\mu A_\nu - W^+_\nu A_\mu) + ig' c_w (W^+_\mu Z_\nu - W^+_\nu Z_\mu|^2 +$$
$$-\frac{1}{4}|\partial_\mu Z_\nu - \partial_\nu Z_\mu + ig' c_w (W^-_\mu W^+_\nu - W^+_\mu W^-_\nu)|^2 +$$
$$-\frac{1}{2} M^2_\eta \eta^2 - \frac{g M^2_\eta}{8 M_W} \eta^3 - \frac{g'^2 M^2_\eta}{32 M_W} \eta^4 + |M_W W^+_\mu + \frac{g}{2} \eta W^+_\mu|^2 +$$
$$+\frac{1}{2}|\partial_\mu \eta + i M_Z Z_\mu + \frac{ig}{2c_w} \eta Z_\mu|^2 - \sum_f \frac{g}{2} \frac{m_f}{M_W} \bar{\Psi}_f \Psi_f \eta$$

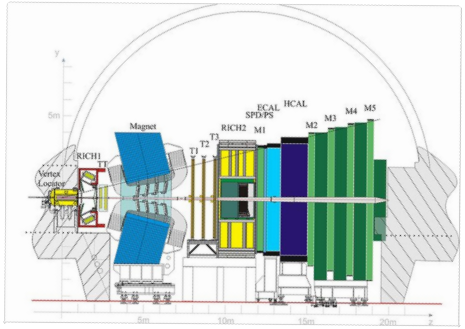

Data Collection

Data Reconstruction

Hypothesis testing

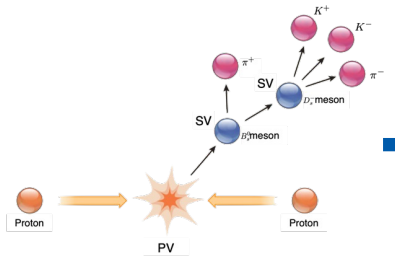

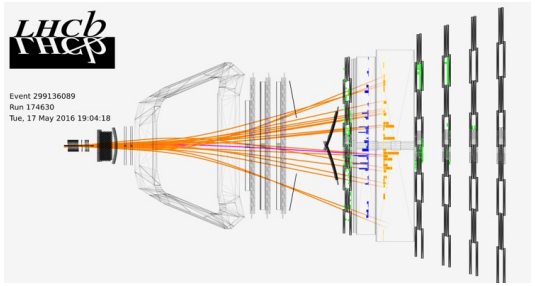

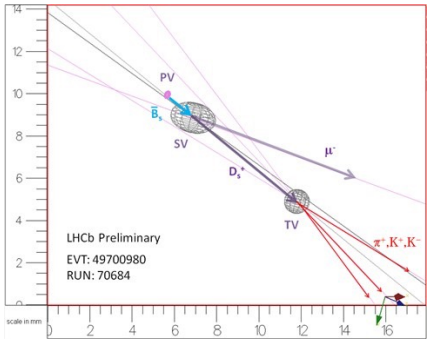

$$\mathcal{L}_{GWS} = \sum_f (\bar{\Psi}_f (i\gamma^\mu \partial\mu - m_f)\Psi_f - eQ_f\bar{\Psi}_f\gamma^\mu\Psi_f A_\mu) +$$
$$+\frac{g}{\sqrt{2}}\sum_i (a_L^i\gamma^\mu b_L^i W_\mu^+ + \bar{b}_L^i\gamma^\mu a_L^i W_\mu^-) + \frac{g}{2c_w}\sum_f \bar{\Psi}_f\gamma^\mu(I_f^3 - 2s_w^2 Q_f - I_f^3\gamma_5)\Psi_f Z_\mu +$$
$$-\frac{1}{4}|\partial_\mu A_\nu - \partial_\nu A_\mu - ie(W_\mu^- W_\nu^+ - W_\mu^+ W_\nu^-)|^2 - \frac{1}{2}|\partial_\mu W_\nu^+ - \partial_\nu W_\mu^+ +$$
$$-ie(W_\mu^+ A_\nu - W_\nu^+ A_\mu) + ig' c_w(W_\mu^+ Z_\nu - W_\nu^+ Z_\mu|^2 +$$
$$-\frac{1}{4}|\partial_\mu Z_\nu - \partial_\nu Z_\mu + ig' c_w(W_\mu^- W_\nu^+ - W_\mu^+ W_\nu^-)|^2 +$$
$$-\frac{1}{2}M_\eta^2\eta^2 - \frac{gM_\eta^2}{8M_W}\eta^3 - \frac{g'^2 M_\eta^2}{32M_W}\eta^4 + |M_W W_\mu^+ + \frac{g}{2}\eta W_\mu^+|^2 +$$
$$+\frac{1}{2}|\partial_\mu\eta + iM_Z Z_\mu + \frac{ig}{2c_w}\eta Z_\mu|^2 - \sum_f \frac{g}{2}\frac{m_f}{M_W}\bar{\Psi}_f\Psi_f\eta$$

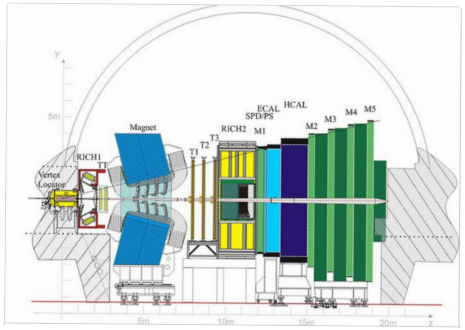

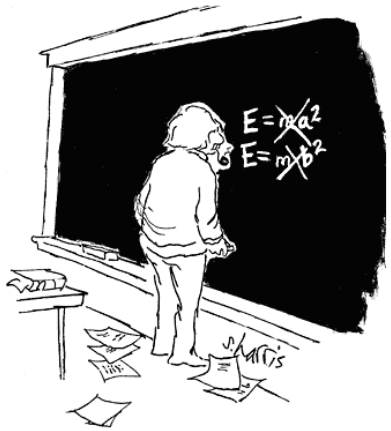

Data Collection

Data Reconstruction

Hypothesis testing

Tuning the process

t, ₽ → min

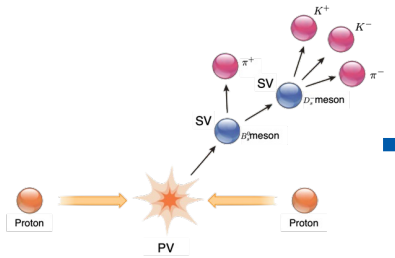

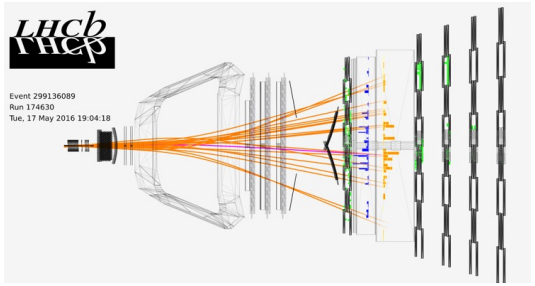

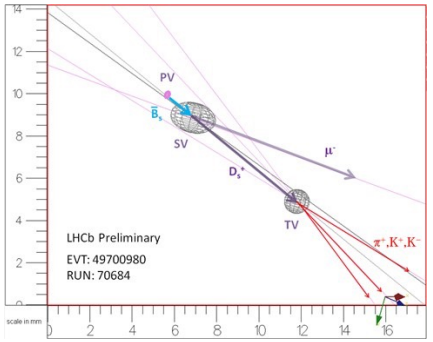

$$\mathcal{L}_{GWS} = \sum_f (\bar{\Psi}_f (i\gamma^\mu \partial\mu - m_f)\Psi_f - eQ_f \bar{\Psi}_f \gamma^\mu \Psi_f A_\mu) +$$
$$+\frac{g}{\sqrt{2}} \sum_i (\bar{a}^i_L \gamma^\mu b^i_L W^+_\mu + \bar{b}^i_L \gamma^\mu a^i_L W^-_\mu) + \frac{g}{2c_w} \sum_f \bar{\Psi}_f \gamma^\mu (I^3_f - 2s^2_w Q_f - I^3_f \gamma_5) \Psi_f Z_\mu +$$
$$-\frac{1}{4}|\partial_\mu A_\nu - \partial_\nu A_\mu - ie(W^-_\mu W^+_\nu - W^+_\mu W^-_\nu)|^2 - \frac{1}{2}|\partial_\mu W^+_\nu - \partial_\nu W^+_\mu +$$
$$-ie(W^+_\mu A_\nu - W^+_\nu A_\mu) + ig' c_w (W^+_\mu Z_\nu - W^+_\nu Z_\mu|^2 +$$
$$-\frac{1}{4}|\partial_\mu Z_\nu - \partial_\nu Z_\mu + ig' c_w (W^-_\mu W^+_\nu - W^+_\mu W^-_\nu)|^2 +$$
$$-\frac{1}{2} M^2_\eta \eta^2 - \frac{g M^2_\eta}{8 M_W} \eta^3 - \frac{g'^2 M^2_\eta}{32 M_W} \eta^4 + |M_W W^+_\mu + \frac{g}{2} \eta W^+_\mu|^2 +$$
$$+\frac{1}{2}|\partial_\mu \eta + i M_Z Z_\mu + \frac{ig}{2c_w} \eta Z_\mu|^2 - \sum_f \frac{g}{2} \frac{m_f}{M_W} \bar{\Psi}_f \Psi_f \eta$$

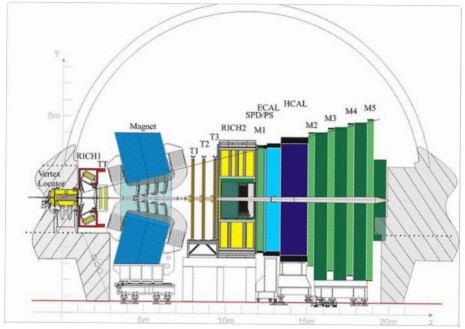

Data Collection

Data Reconstruction

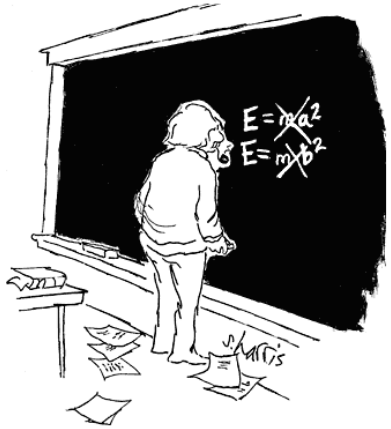

Hypothesis testing

Tunable Data Analysis

t, ₽ → min

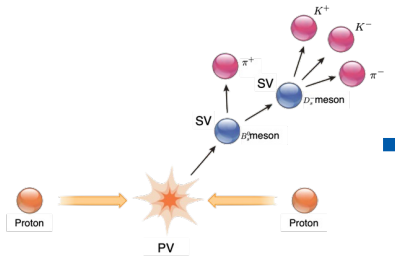

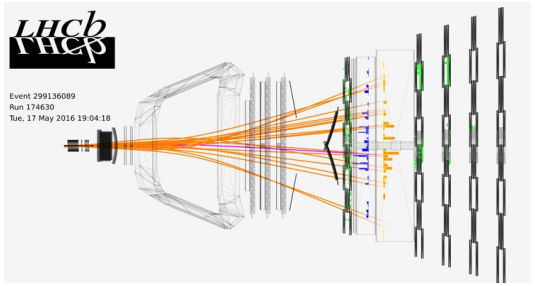

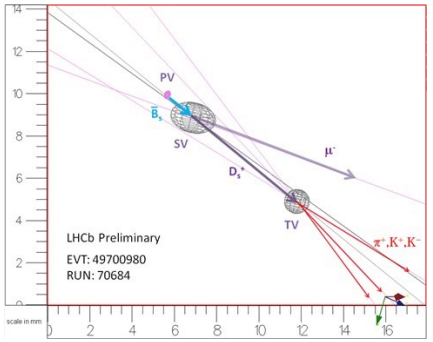

$$\mathcal{L}_{GWS} = \sum_f (\bar{\Psi}_f (i\gamma^\mu \partial\mu - m_f)\Psi_f - eQ_f \bar{\Psi}_f \gamma^\mu \Psi_f A_\mu) +$$
$$+\frac{g}{\sqrt{2}} \sum_i (\bar{a}^i_L \gamma^\mu b^i_L W^+_\mu + \bar{b}^i_L \gamma^\mu a^i_L W^-_\mu) + \frac{g}{2c_w} \sum_f \bar{\Psi}_f \gamma^\mu (I^3_f - 2s^2_w Q_f - I^3_f \gamma_5) \Psi_f Z_\mu +$$
$$-\frac{1}{4}|\partial_\mu A_\nu - \partial_\nu A_\mu - ie(W^-_\mu W^+_\nu - W^+_\mu W^-_\nu)|^2 - \frac{1}{2}|\partial_\mu W^+_\nu - \partial_\nu W^+_\mu +$$
$$-ie(W^+_\mu A_\nu - W^+_\nu A_\mu) + ig' c_w (W^+_\mu Z_\nu - W^+_\nu Z_\mu|^2 +$$
$$-\frac{1}{4}|\partial_\mu Z_\nu - \partial_\nu Z_\mu + ig' c_w (W^-_\mu W^+_\nu - W^+_\mu W^-_\nu)|^2 +$$
$$-\frac{1}{2} M^2_\eta \eta^2 - \frac{g M^2_\eta}{8 M_W} \eta^3 - \frac{g'^2 M^2_\eta}{32 M_W} \eta^4 + |M_W W^+_\mu + \frac{g}{2} \eta W^+_\mu|^2 +$$
$$+\frac{1}{2}|\partial_\mu \eta + i M_Z Z_\mu + \frac{ig}{2c_w} \eta Z_\mu|^2 - \sum_f \frac{g}{2} \frac{m_f}{M_W} \bar{\Psi}_f \Psi_f \eta$$

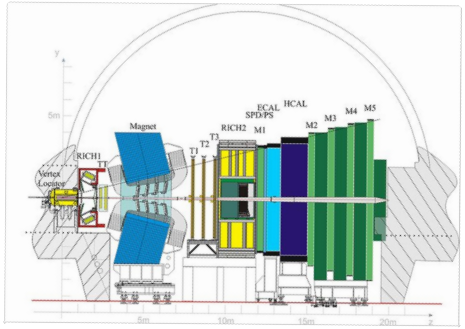

Data Collection

Data Reconstruction

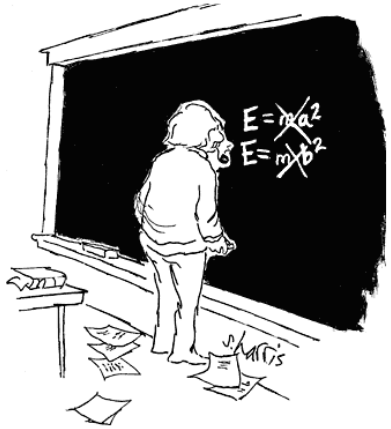

Hypothesis testing

Analyzing the Inputs

t, ₽ → min

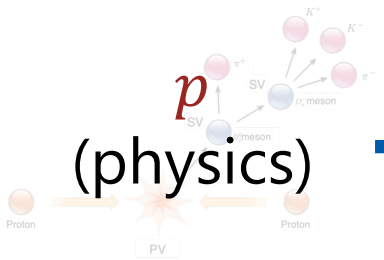

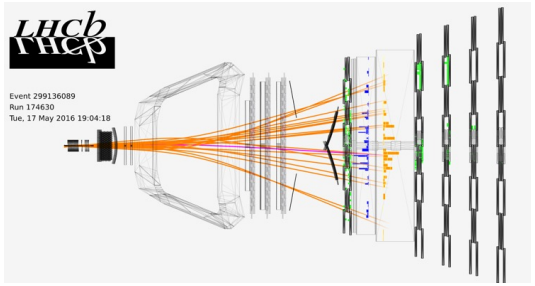

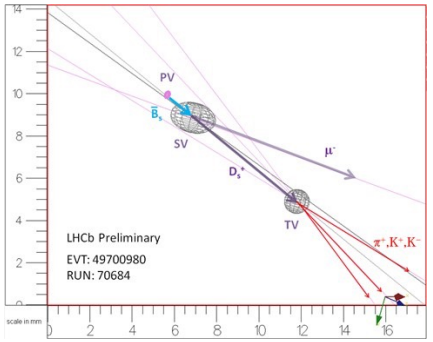

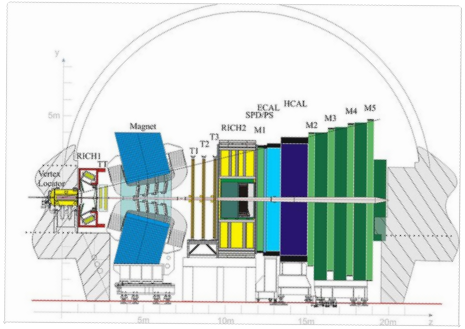

Data Collection

Data Reconstruction

Building the Detector

t, ₽ → min

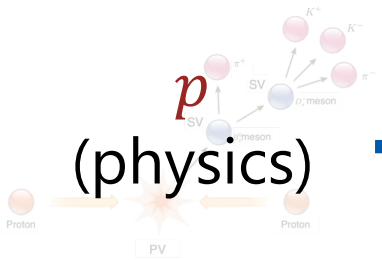

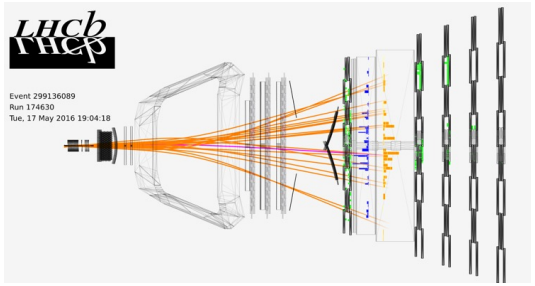

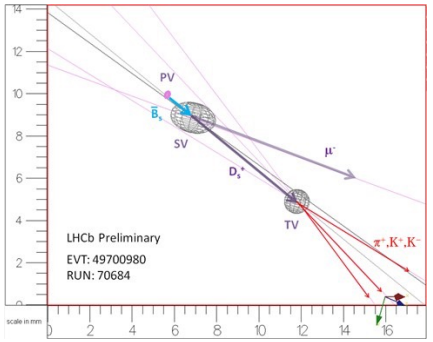

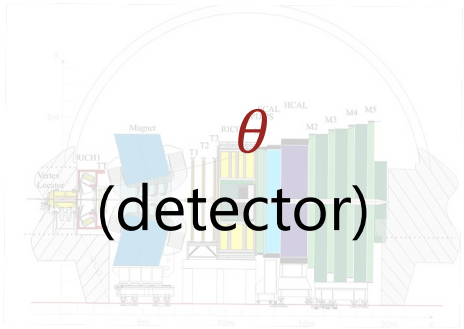

Data Collection

Data Reconstruction

Obtaining the data

t, ₽ → min

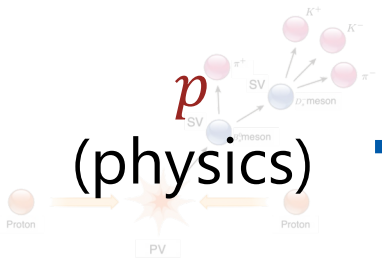

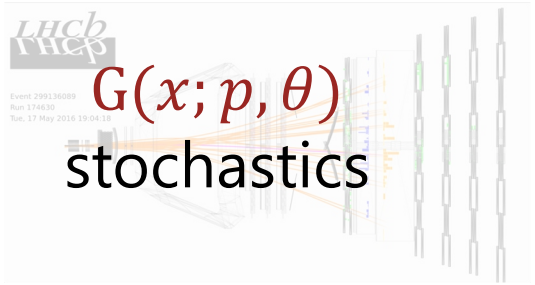

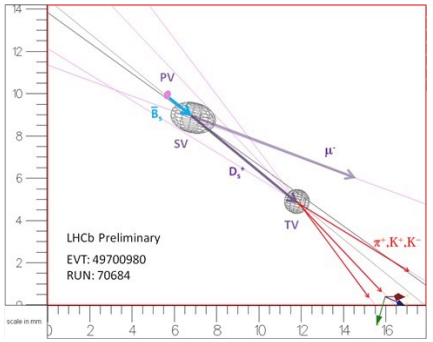

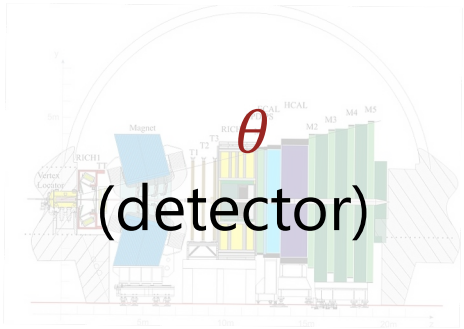

Data Collection

Data Reconstruction

Understanding the data

t, ₽ → min

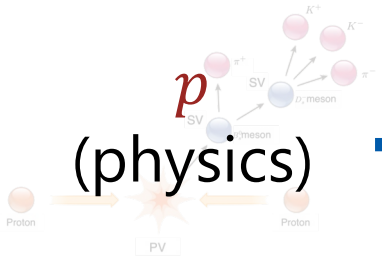

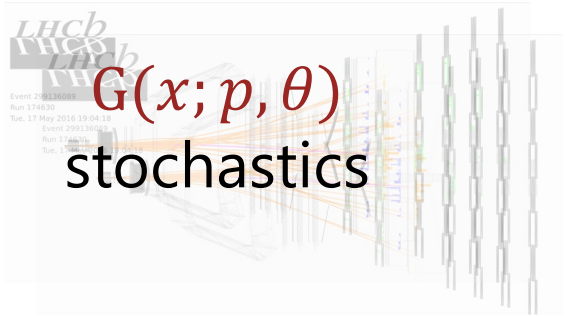

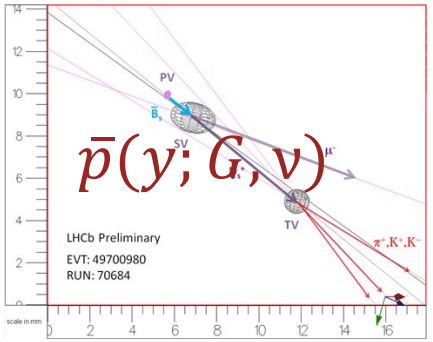

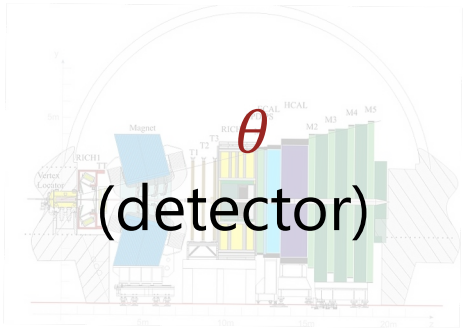

Data Collection

Data Reconstruction

Best performance metrics

t, ₽ → min

$< (p - \bar{p})^2 >$

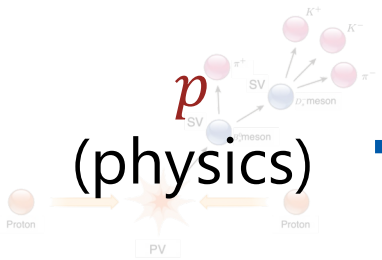

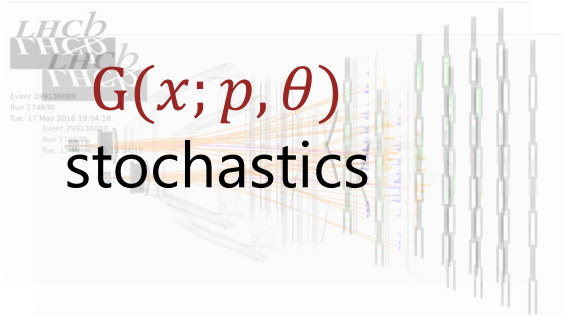

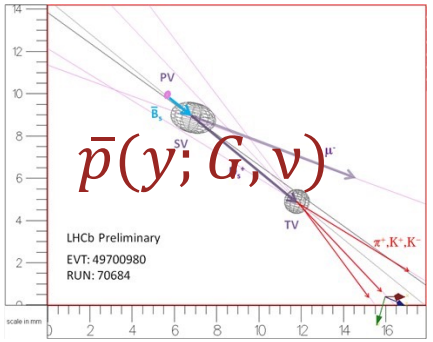

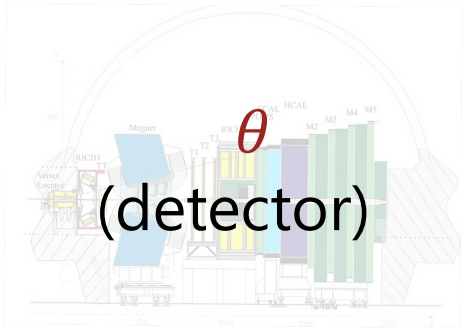

Data Collection

Data Reconstruction

Minimizing the cost

t → min

$< (p - \bar{p})^2 >$

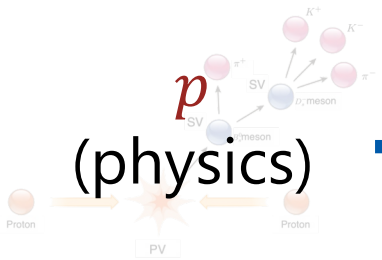

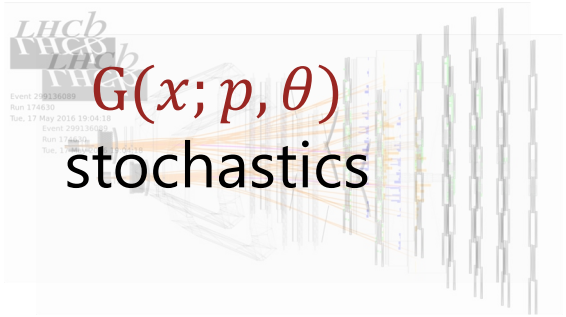

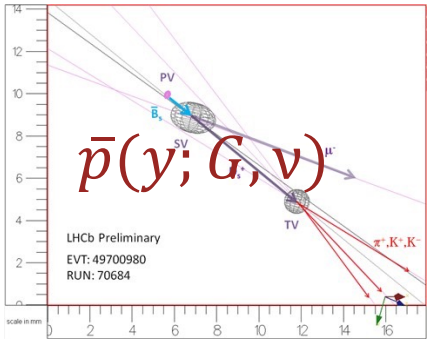

$$L(\text{₽}) \sim exp(\text{₽}_{\text{fix}} - \text{₽})$$

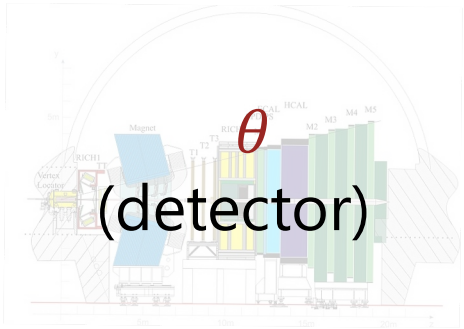

Data Collection

Data Reconstruction

Minimizing the Time

Automate

$< (p - \bar{p})^2 >$

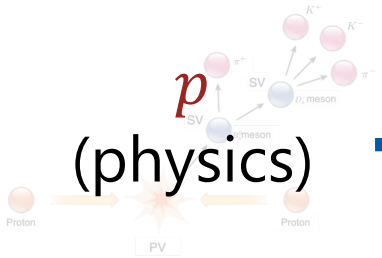

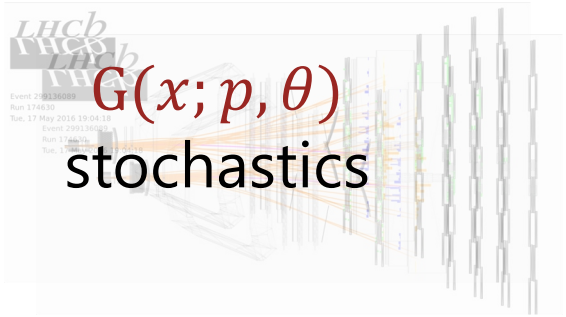

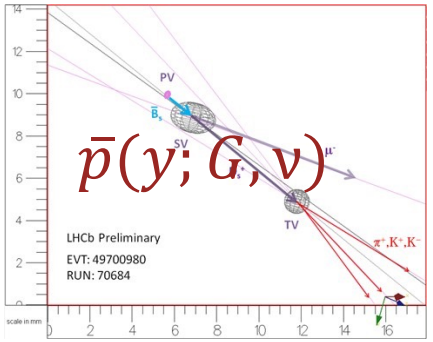

$L \sim exp(\mathbf{P}_{\text{fix}} - \mathbf{P})$

$\mathbf{P} = \mathbf{P}(\theta)$

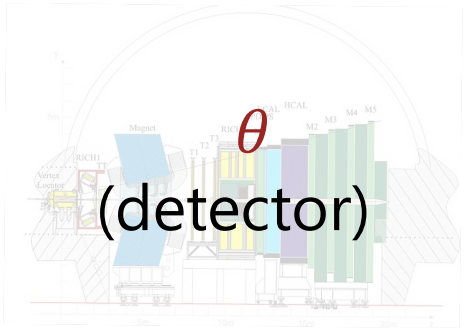

SIMULATION

Data Reconstruction

Difficulties

Automate

$L \sim exp(₱_{\text{fix}} - ₱)$ $< (p - \bar{p})^2 >$

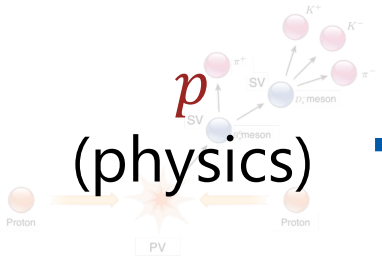

p
(physics)

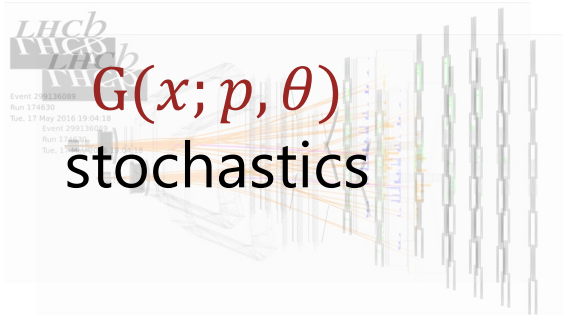

$G(x; p, \theta)$
stochastics

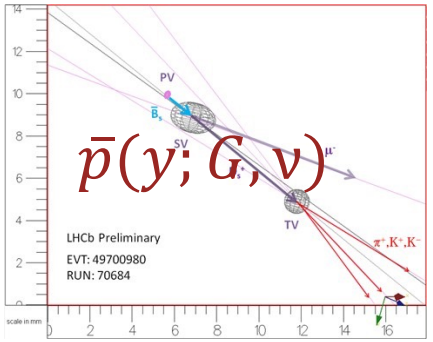

$\bar{p}(y; G, \nu)$

- $G(x; p, \theta)$ physics simulator ~1event/minute
- ν chosen manually
- L not differentiable

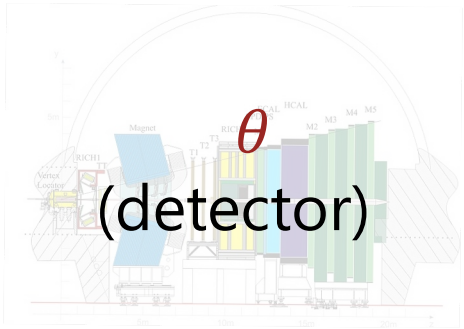

θ
(detector)

ν
(algorithm)

SIMULATION

Data Reconstruction

Forward Problem

Simulation $\mathrm{G}(x; p, \theta)$

Several model-motivated transitions.

Sequence:

- collision;
- decay;
- matter interaction;
- digitisation;
- reconstruction.

Each event takes 1 minute to generate (real world data is "generated" at several MHz).

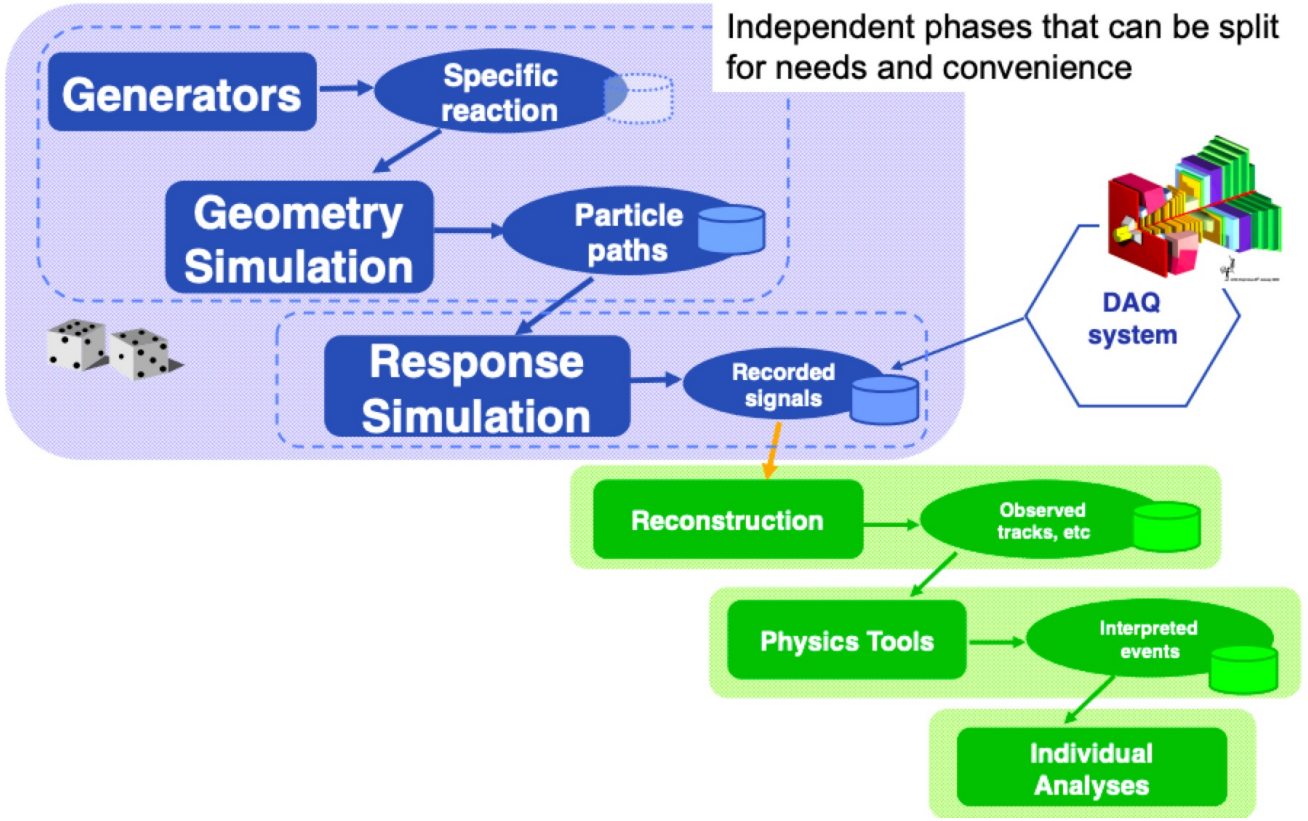

Simulate "simulation" using effective parameterization.

What is the event.

The calorimeter consists of many cells that reads out the energy deposit of a single particle.

The LHCb calorimeter construction motivated by the need to have better performance in the most populated regions.

A single particle deposits energy to several cells. An event is a sum of all particles and some noise.

We are normally in some reconstructed parameters of the event.

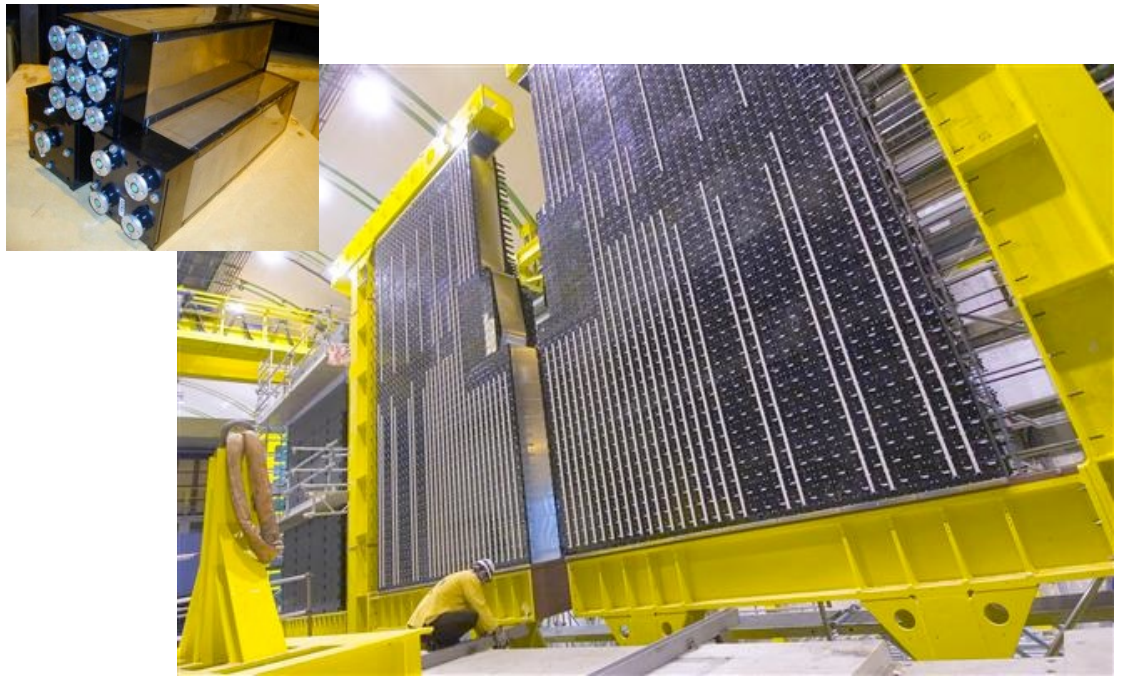

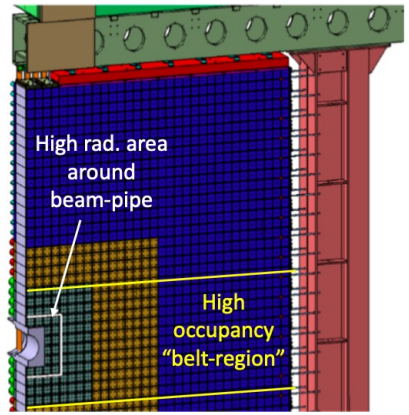

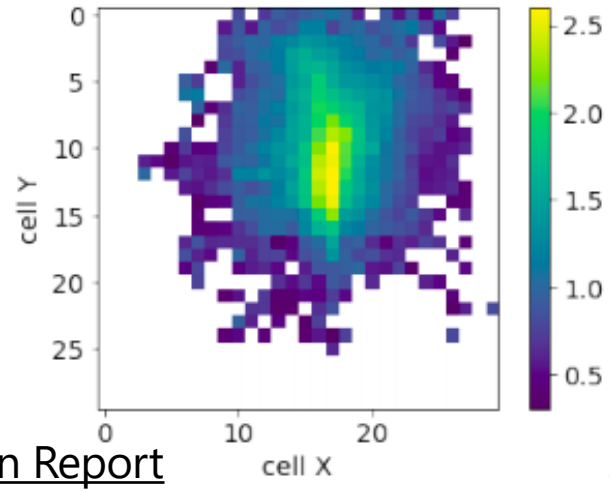

LHCb Calorimeter Technical Design Report

Ideas for Simulation

Since we know all processes in the subdetector, we can fully simulate an event using precise physics-motivated rules.

For calorimeters this means taking into account the structure of response that consists of many secondary particles.

This is done using Geant toolkit.

Pro: physics behind the simulation is controlled
Cons: slow, needs fine tuning.

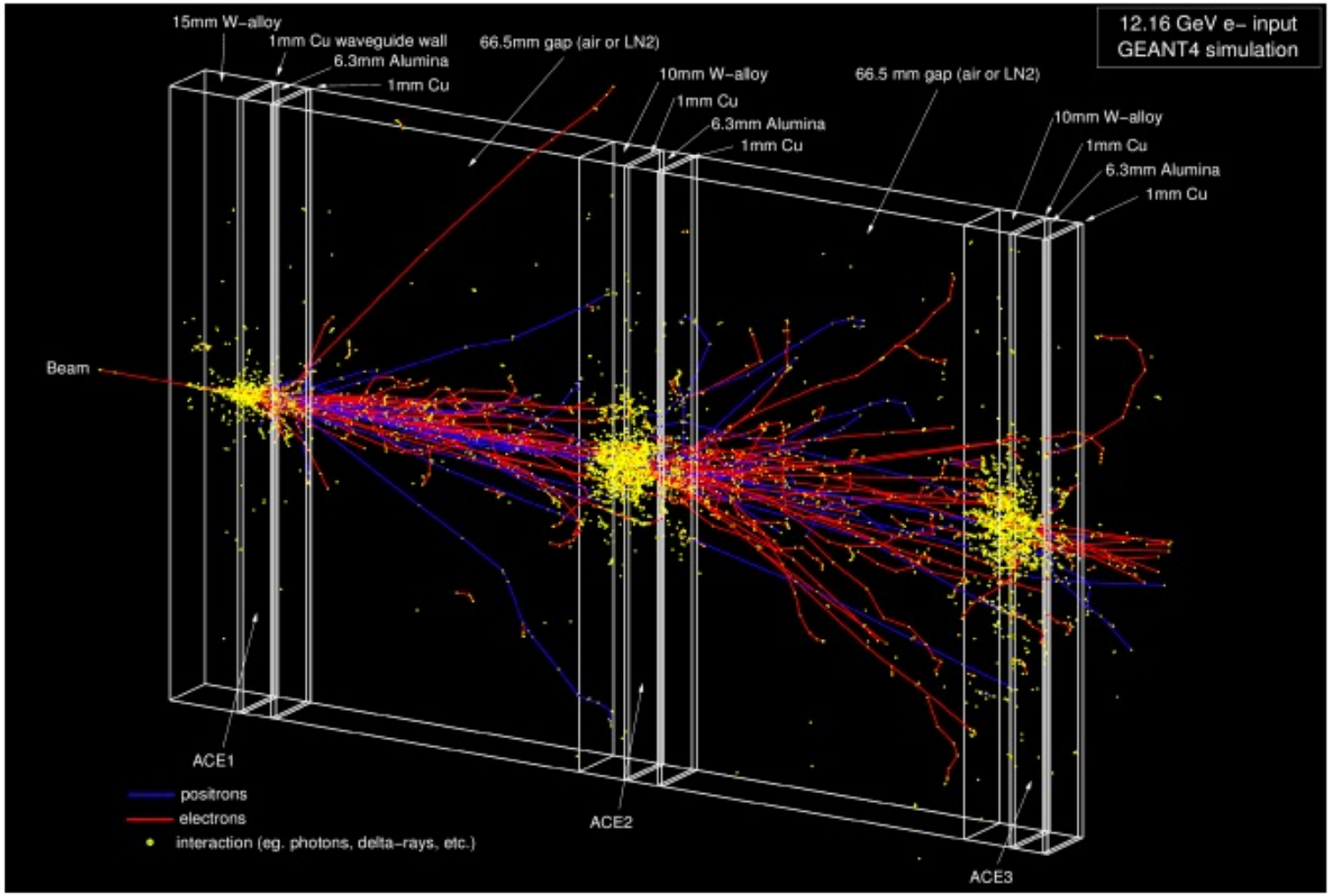

FIG. 2: Layout diagram, and GEANT4 simulation of a single 12.16 GeV electron event in our ACE detector system; in this case liquid nitrogen occupies the interelement spaces.

Ideas for Tabular Methods

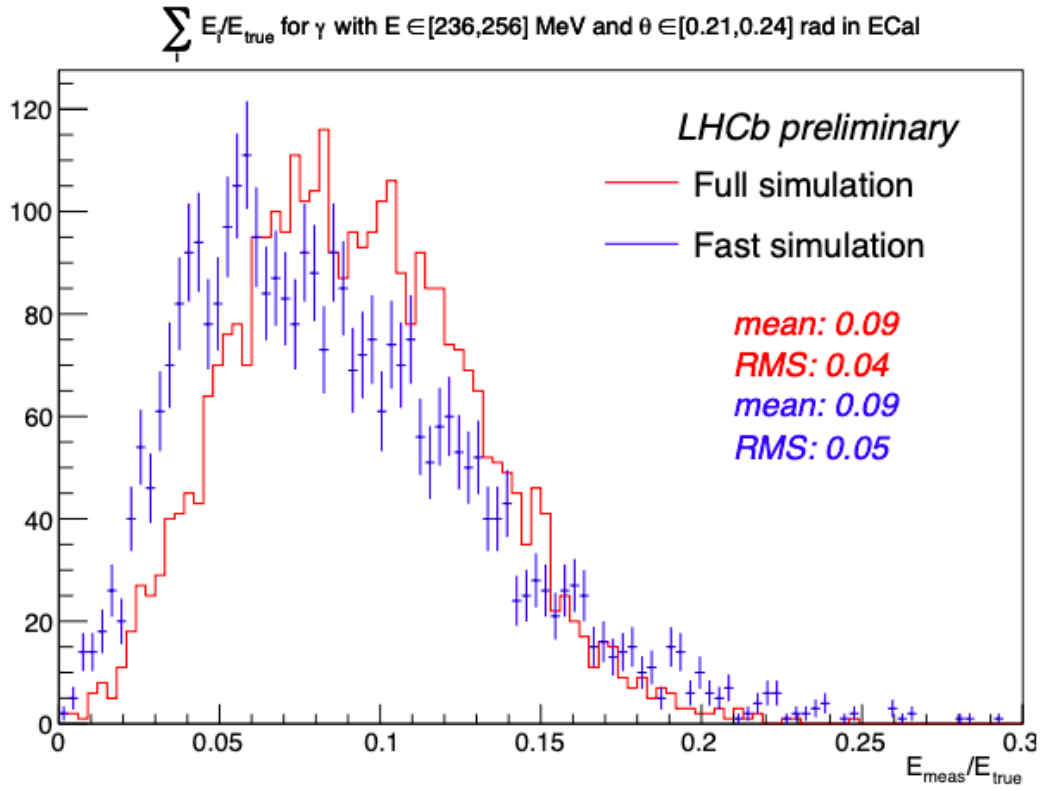

Build a library of calorimeter responses to impact particle in corresponding 5D phase space using GEANT4 («frozen showers»).

5D = 3D momentum + 2D coordinate for every particle type.

The whole phase space is split into bins, the exact observable is obtained interpolating between the bins.

One can also construct full interpolation (without using bins).

Pros: easy to interpret, quality is controlled by the number of samples.

Cons: curse of dimensionality, memory consumption, full interpolation takes huge efforts.

Making it continuous

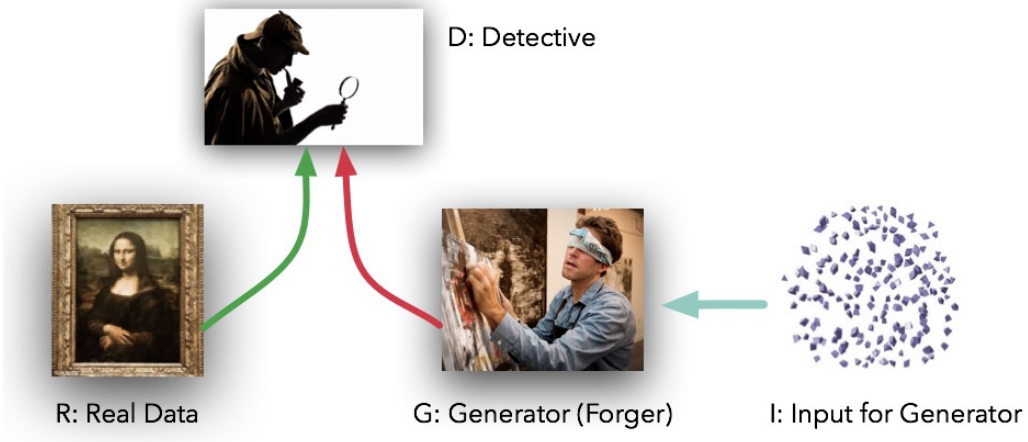

We can try to use the recent concept of Generative adversarial network, that can be characterised by the interplay between a forger and a detective.

At the Large Hadron Collider, nature is an artist. We need to learn how to fake these paintings.

Generative modeling $\mathrm{G}(x; p, \theta)$

- **Conditional** dependence on detector parameters $\boldsymbol{\theta}$ and incident particle information $\boldsymbol{p}$.

Need to be
- Tunable.
- Robust.
- Fast for sampling.

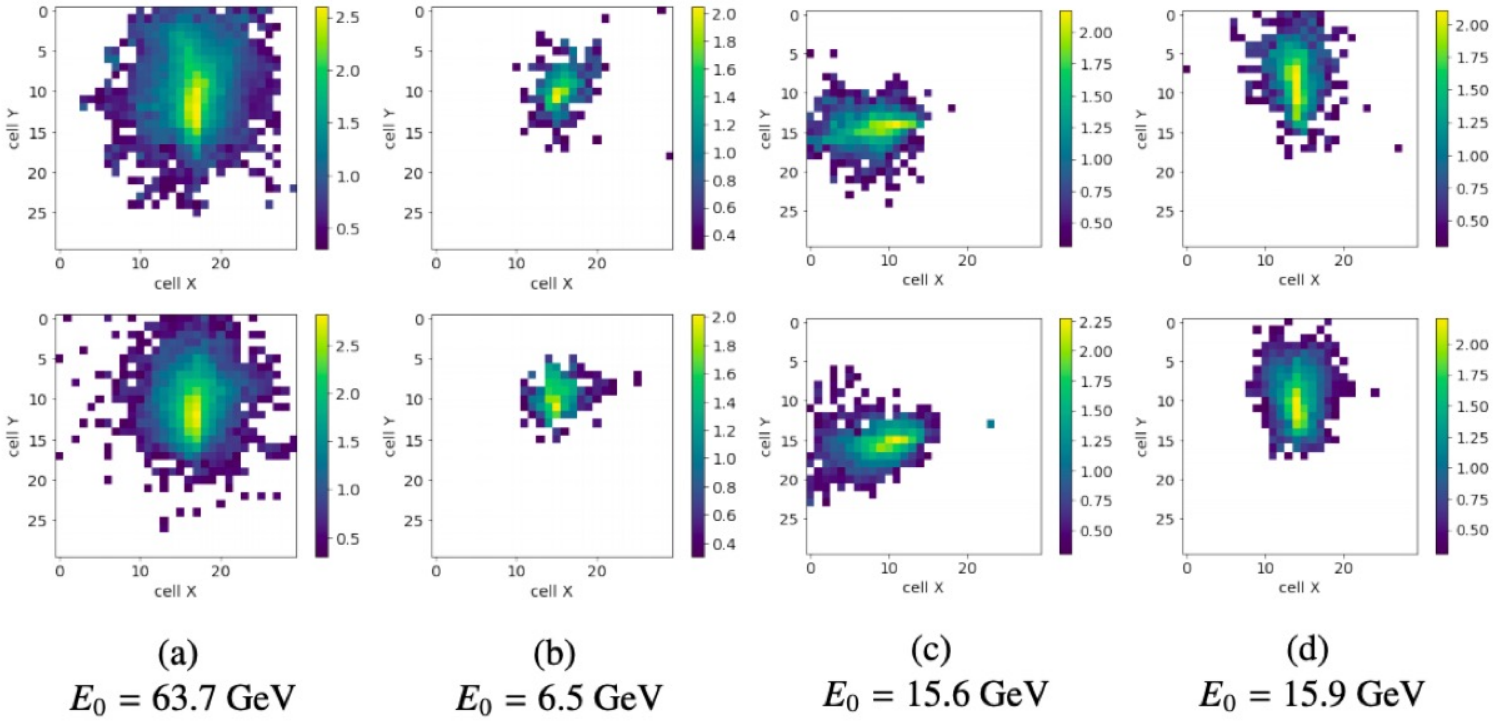

(a) $E_0 = 63.7$ GeV (b) $E_0 = 6.5$ GeV (c) $E_0 = 15.6$ GeV (d) $E_0 = 15.9$ GeV

V. Chekalina et al. *EPJ Web Conf.* 214 (2019) 02034

Challenges: Implementations

More challenges:

- **Distilling the generators.**
  Aim: beyond 100ms/event.

- **Testing the generator quality in the limit of small data samples.**
  Aim: on-the-fly algorithms.

- **Implementing pipeline in the online environment (200xNVidia RTX A5000 from LHCb).**
  Aim: Efficient architecture and Scheduling given resources.

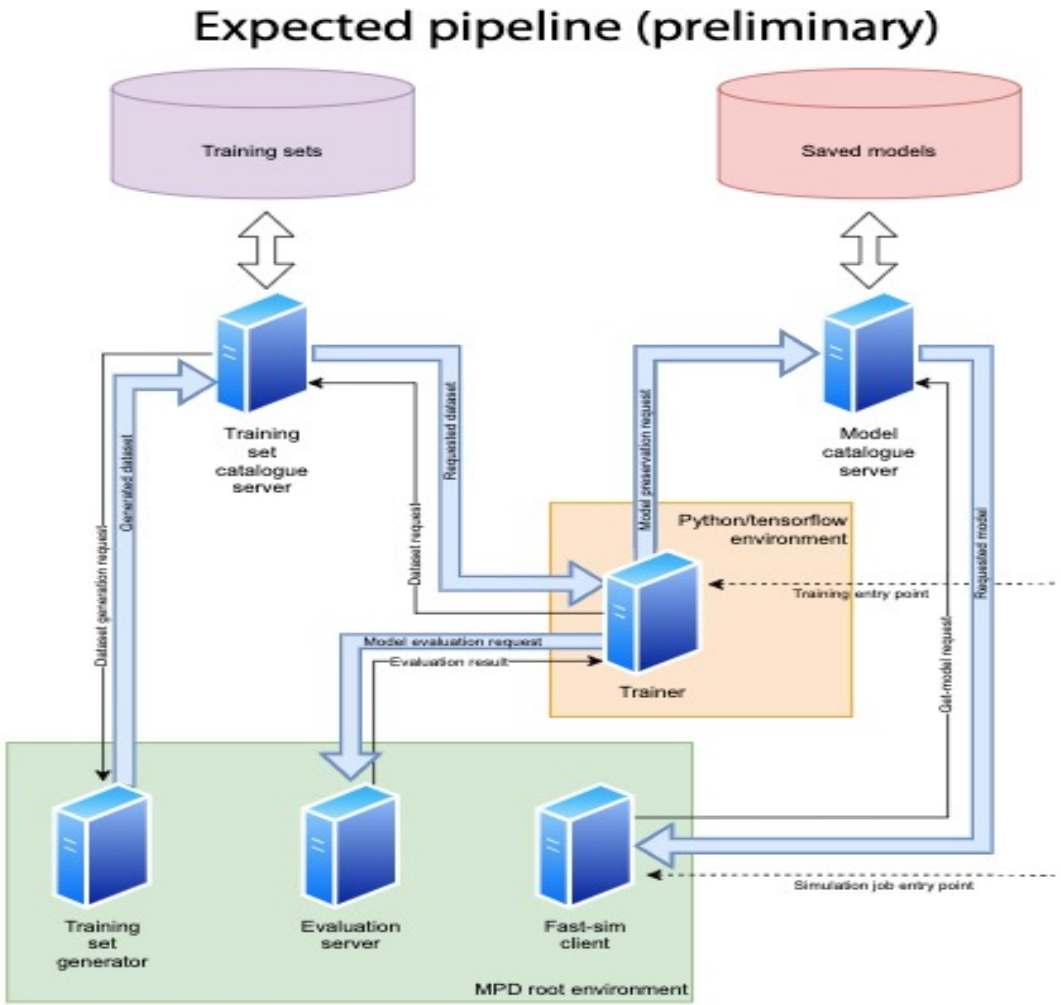

D. Zolotukhin (BSc Diploma)
R. Drynkin (BSc Diploma)

Inverse Problem

Reconstruction $\nu = \nu(\theta)$

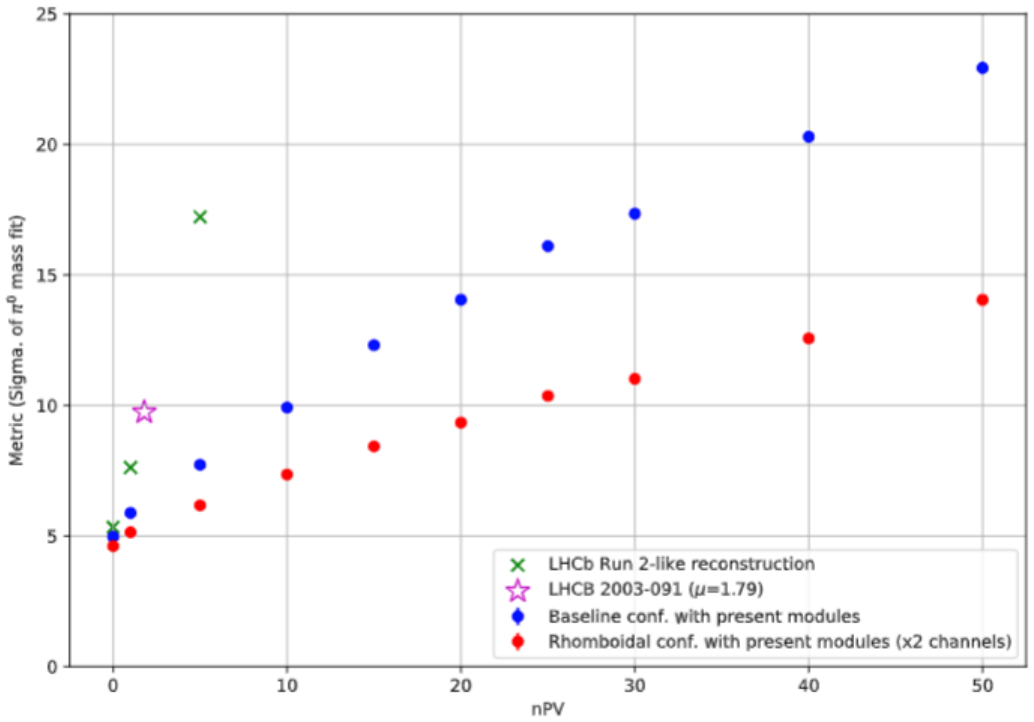

Need to "get rid" of experts help in inverse problem

Current solution:

- Self-trained solution for every point from θ;
- Challenge: universal training for many points of θ.

A Boldyrev et al. 2020 JINST 15 C09030

Difficulties

Automate

$L \sim exp(\text{₱}_{\text{fix}} - \text{₱})^2 < (p - \bar{p})^2 >$

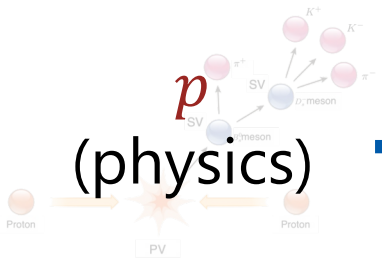

p
(physics)

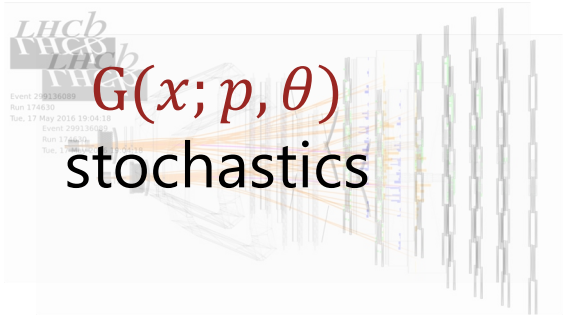

$G(x; p, \theta)$
stochastics

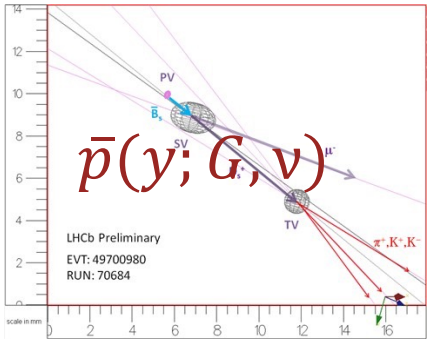

$\bar{p}(y; G, \nu)$

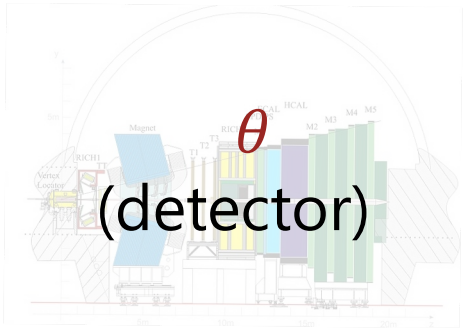

θ
(detector)

ν
(algorithm)

- ~~$G(x; p, \theta)$ physics simulator ~1event/minute~~

- ~~ν chosen manually~~

- L not differentiable

SIMULATION Data Reconstruction

Surrogates

Black box optimization

$$L \sim exp(₽_{\text{fix}} - ₽)^2 < (p - \bar{p})^2 >$$

- The value at any point is known.
- The analytical formula is unknown.
- The time to compute the value is several tens of hours.
- Classical black-box optimization problem:
  - Optimizing someone else's code (there is only a compiled library).
  - Systems described by differential equations (airplane wing shape).

Black Box Solution

- Expert Method
  - Might be wrong
- Random search.
  - Works sometimes.
- Surrogate modeling

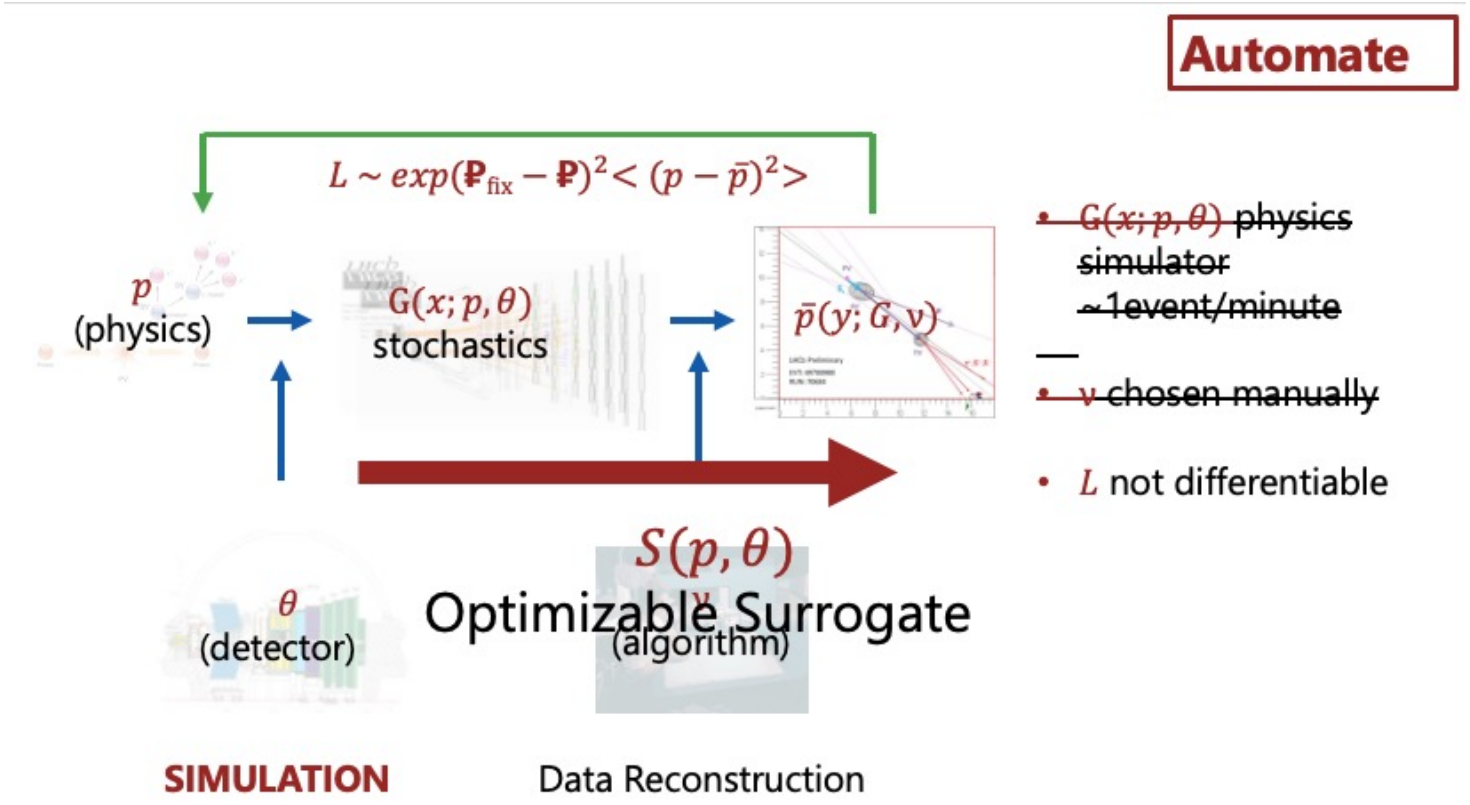

SHiP Experiment Design

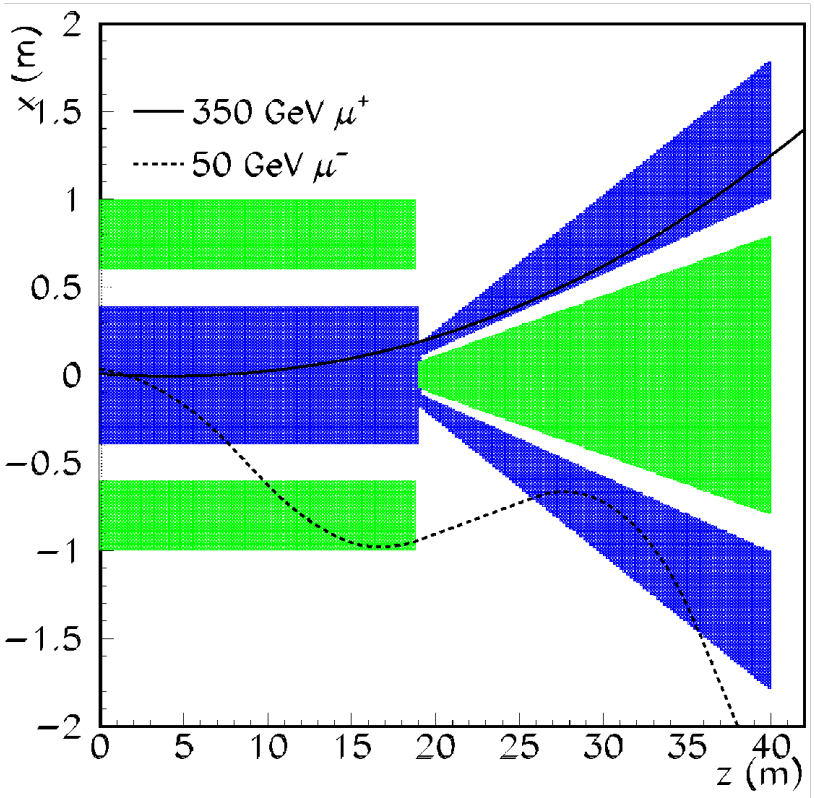

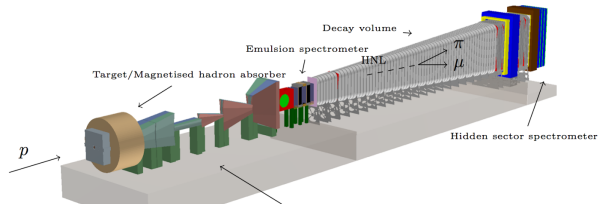

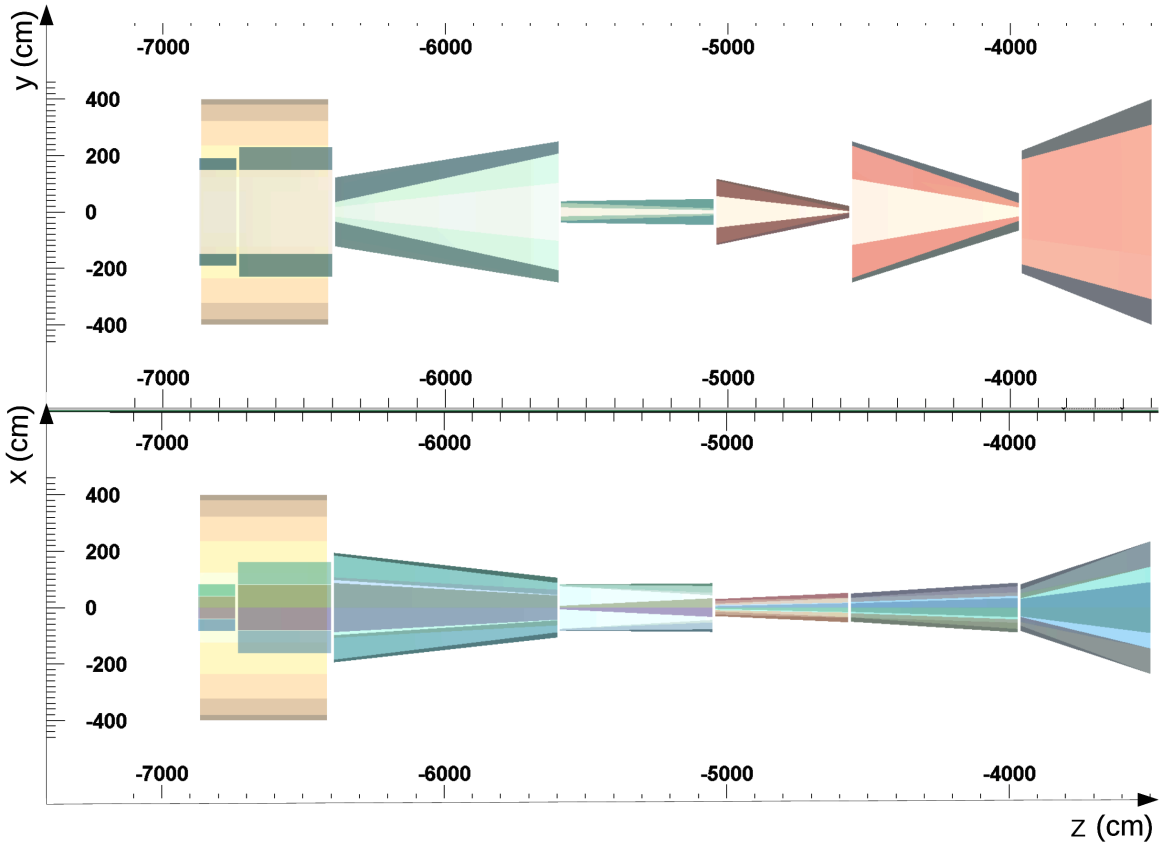

- Absorber shape optimization: background suppression at reasonable cost

Final Optimization

Surrogate modeling using Bayesian Optimization of Gaussian Processes.

Optimization brought 25% cheaper solution.

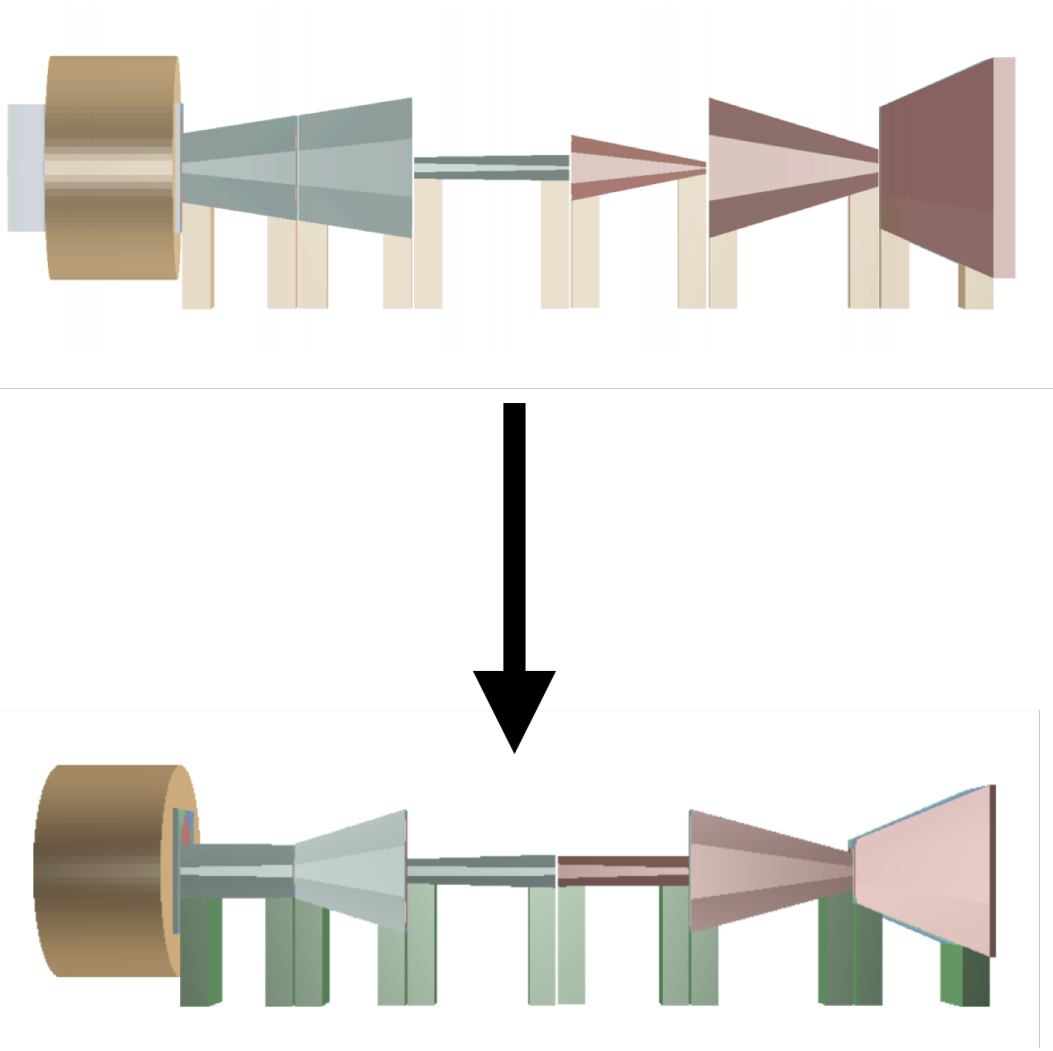

Forbes Рубрики Рейтинги Видео Life Woma

Trivio Блог

Мастер-класс от Trivio: как в ситуации форс-мажора держать сервис на высоте

Новости 23.09.2022

20 марта 2018 г. · Технологии

Поймать темную материю: как российские ученые сэкономили ЦЕРН более $1 млн

Екатерина Кинякина
Автор

Копировать ссылку

A. Filatov et al. Journal of Physics: Conference Series. 2017. Vol. 934. P. 1-5

Conclusions

- Optimization of large setups requires simultaneous approximate fast solutions of forward and inverse problems.
- Final stage of the optimization needs precise surrogate modeling.
- A complete optimization cycle brings in significant reduction in costs (and thus efficiencies) but requires several fundamental questions to be solved.
- Future outlook:
  - Many areas to be re-explored using new (data-driven) machine-learning approaches.
  - Many areas are already re-explored (https://mode-collaboration.github.io/)

Conclusions

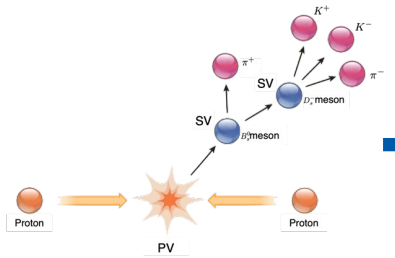

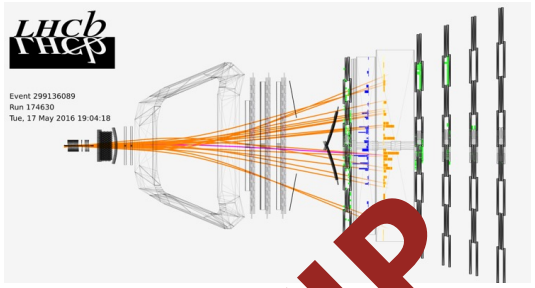

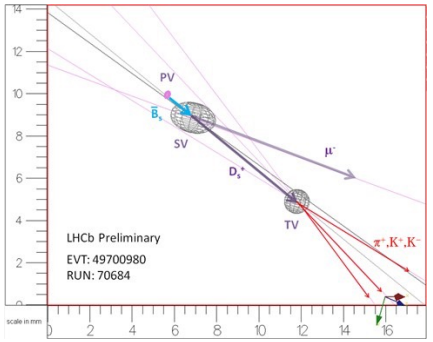

$$\mathcal{L}_{GWS} = \sum_f (\bar{\Psi}_f (i\gamma^\mu \partial\mu - m_f)\Psi_f - eQ_f \bar{\Psi}_f \gamma^\mu \Psi_f A_\mu) +$$
$$+\frac{g}{\sqrt{2}} \sum_i (a_L^i \gamma^\mu b_L^i W_\mu^+ + \bar{b}_L^i \gamma^\mu a_L^i W_\mu^-) + \frac{g}{2c_w} \sum_f \bar{\Psi}_f \gamma^\mu (I_f^3 - 2s_w^2 Q_f - I_f^3 \gamma_5) \Psi_f Z_\mu +$$
$$-\frac{1}{4}|\partial_\mu A_\nu - \partial_\nu A_\mu - ie(W_\mu^- W_\nu^+ - W_\mu^+ W_\nu^-)|^2 - \frac{1}{2}|\partial_\mu W_\nu^+ - \partial_\nu W_\mu^+ +$$
$$-ie(W_\mu^+ A_\nu - W_\nu^+ A_\mu) + ig' c_w (W_\mu^+ Z_\nu - W_\nu^+ Z_\mu|^2 +$$
$$-\frac{1}{4}|\partial_\mu Z_\nu - \partial_\nu Z_\mu + ig' c_w (W_\mu^- W_\nu^+ - W_\mu^+ W_\nu^-)|^2 +$$
$$-\frac{1}{2} M_\eta^2 \eta^2 - \frac{g M_\eta^2}{8 M_W} \eta^3 - \frac{g'^2 M_\eta^2}{32 M_W} \eta^4 + |M_W W_\mu^+ + \frac{g}{2} \eta W_\mu^+|^2 +$$
$$+\frac{1}{2}|\partial_\mu \eta + i M_Z Z_\mu + \frac{ig}{2c_w} \eta Z_\mu|^2 - \sum_f \frac{g}{2} \frac{m_f}{M_W} \bar{\Psi}_f \Psi_f \eta$$

WIP

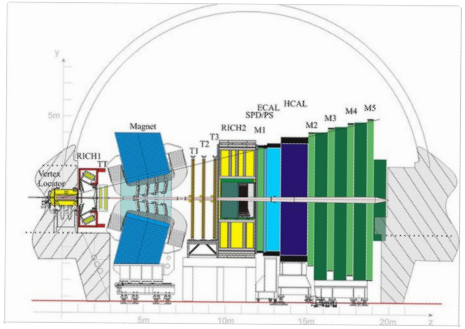

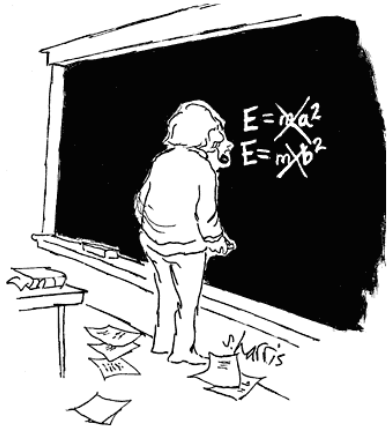

Сбор данных

Реконструкция

Проверка гипотез

Conclusions

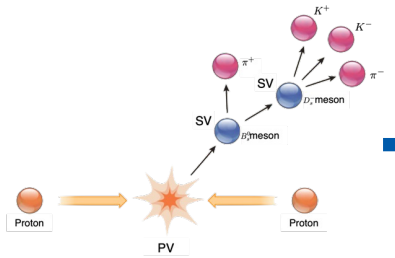

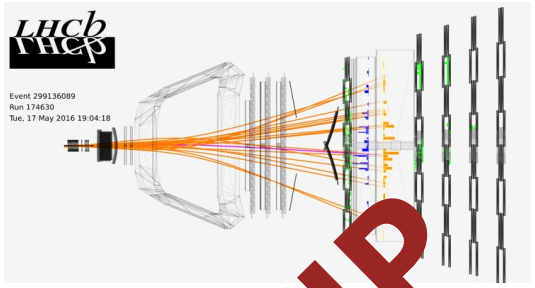

WIP

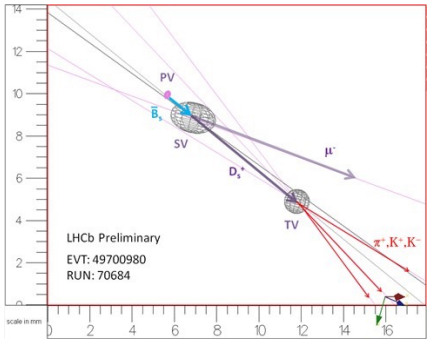

$$\mathcal{L}_{GWS} = \sum_f (\bar{\Psi}_f (i\gamma^\mu \partial\mu - m_f)\Psi_f - eQ_f \bar{\Psi}_f \gamma^\mu \Psi_f A_\mu) +$$
$$+ \frac{g}{\sqrt{2}} \sum_i (a_L^i \gamma^\mu b_L^i W_\mu^+ + \bar{b}_L^i \gamma^\mu a_L^i W_\mu^-) + \frac{g}{2c_w} \sum_f \bar{\Psi}_f \gamma^\mu (I_f^3 - 2s_w^2 Q_f - I_f^3 \gamma_5) \Psi_f Z_\mu +$$
$$- \frac{1}{4}|\partial_\mu A_\nu - \partial_\nu A_\mu - ie(W_\mu^- W_\nu^+ - W_\mu^+ W_\nu^-)|^2 - \frac{1}{2}|\partial_\mu W_\nu^+ - \partial_\nu W_\mu^+ +$$
$$- ie(W_\mu^+ A_\nu - W_\nu^+ A_\mu) + ig' c_w (W_\mu^+ Z_\nu - W_\nu^+ Z_\mu|^2 +$$
$$- \frac{1}{4}|\partial_\mu Z_\nu - \partial_\nu Z_\mu + ig' c_w (W_\mu^- W_\nu^+ - W_\mu^+ W_\nu^-)|^2 +$$
$$- \frac{1}{2} M_\eta^2 \eta^2 - \frac{g M_\eta^2}{8 M_W} \eta^3 - \frac{g'}{32} \eta^4 - |M_W W_\mu^+ + \frac{g}{2} \eta W_\mu^+|^2 +$$
$$+ \frac{1}{2}|\partial_\mu \eta + i M_Z Z_\mu - \frac{ig}{2} \eta Z - \sum_f \frac{g}{2} \frac{m_f}{M_W} \bar{\Psi}_f \Psi_f \eta$$

WIP

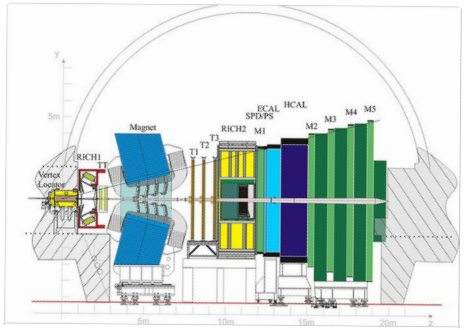

Проверка гипотез